Kinetics and Mechanism of the Iron(III)-Catalyzed Autoxidation of Sulfur(IV) Oxides in Aqueous Solution. Evidence for the Redox Cycling of Iron in the Presence of Oxygen and Modeling of the Overall Reaction Mechanism

Christian Brandt, István Fábián,† and Rudi van Eldik*

Institute for Inorganic Chemistry, University of Witten/Herdecke, 58448 Witten, Germany

Received September 2, 1992®

Kinetic traces for the redox decomposition of iron(III)–sulfito complexes exhibit a peculiar break in the presence of oxygen. A detailed kinetic analysis of this feature as a function of [Fe(III)], [Fe(II)], [S(IV)], and [O_2] at pH 2.5 indicated that this step is a result of the sulfite-induced autoxidation of produced iron(II) in the presence of oxygen. The so observed redox cycling of iron comes to a dead end at the point in time when all the oxygen in the solution has been used up. The kinetic traces can be interpreted in terms of a first-order decay of the iron(III)–sulfito complexes and a reverse pseudo-zero-order oxidation of iron(II) by $SO_5^{\bullet-}$, HSO_5^-, and $SO_4^{\bullet-}$. The latter species are generated in solution via the reaction of $SO_3^{\bullet-}$, produced during the reduction of iron(III) by sulfite, with oxygen. Radical scavengers do not affect the first-order decay but inhibit the pseudo-zero-order step. The results reveal no evidence for the formation of an intermediate oxygenated complex, and clearly indicate the important role of the sulfite-induced redox cycling of iron(II/III) in the presence of oxygen. Computer simulations based on the proposed reaction mechanism are in good agreement with the observed experimental kinetic traces and indicate that the formation of the $SO_5^{\bullet-}$ radical is the main oxygen-consuming step during the overall redox process.

Introduction

The mechanism of the homogeneous transition metal catalyzed oxidation of sulfur(IV) oxides is a subject of contradictory discussion. Three types of mechanisms are discussed in the literature: nonradical,[1-4] radical,[5-12] and combinations of nonradical and radical mechanisms.[13,14] Most of the published radical reactions are based on the mechanism first proposed by Backström[8] in 1934. Evidence for a chain reaction during the transition metal catalyzed oxidation of sulfur(IV) oxides was provided by the observation that radical scavengers like mannitol,[15] *tert*-butyl alcohol,[16] thiosulfate,[17] or hydroquinone[18,19] inhibit the reaction.

In general, these reactions follow a complex mechanism with several distinguishable steps. The initiation step is reportedly the formation of a metal–sulfito complex.[4,5,12,13,18,20-22] Depending on the total [S(IV)], different metal–sulfito complexes are formed.[20,21,23,24] According to earlier results,[21,23,24] iron(III) may form 1:1, 1:2, and 1:3 complexes with HSO_3^-, and the spectrophotometrically observed kinetic curves may represent simultaneous concentration changes of these complexes.

The transition metal–sulfito complexes decompose spontaneously, producing the reduced metal ion and oxidized sulfite species such as the sulfite radical, $SO_3^{\bullet-}$.[22] The decomposition of the iron(III)–sulfito complexes in Ar-saturated solutions has been studied extensively.[23,25] In the absence of oxygen the sulfite radical may participate in various reaction steps during which sulfate, SO_4^{2-}, and dithionate, $S_2O_6^{2-}$, are produced.[23,25] It has been suggested that in Ar-saturated solutions the formation of SO_4^{2-} and $S_2O_6^{2-}$, by the recombination of the $SO_3^{\bullet-}$ radicals, occur in a ratio of ca. 1:1.[26] According to Luňák and Vrepřek-Šiška,[27] the oxidation of iron(II) is also a sink for the sulfite radical. In the presence of oxygen the latter reaction is in competition with the reaction with oxygen, which results in the formation of the peroxomonosulfate radical, $SO_5^{\bullet-}$.[28,29] The formation of SO_3 and $O_2^{\bullet-}$ during the reaction of $SO_3^{\bullet-}$ and O_2 is unlikely.[28] The $SO_5^{\bullet-}$ radical can react with HSO_3^- or iron(II) to produce the hydrogen peroxomonosulfate anion, HSO_5^-.[29,30]

Although most of our earlier work[21,23,25] was performed in Ar-saturated solutions to focus on the iron(III)–sulfur(IV) interaction, some preliminary experiments in the presence of oxygen indicated a significant acceleration effect during the decomposition of the transient iron(III)–sulfur(IV) complexes.[23,25] Contrary to this acceleration effect, most authors find a zero-order dependence on oxygen for the homogeneous iron(III) catalysis[31,32] and a first-order dependence on oxygen for iron(II)

† On leave from the Department of Inorganic and Analytical Chemistry, Lajos Kossuth University, H-4010 Debrecen, Hungary.

* Abstract published in *Advance ACS Abstracts,* January 1, 1994.

(1) Bassett, H.; Parker, W. A. *J. Chem. Soc.* **1951**, 1540.
(2) Freiberg, J. *Atmos. Environ.* **1975**, *9*, 661.
(3) Luňák, S.; El-Wakil, A. M.; Vepřek-Šiška, J. *Collect. Czech. Chem. Commun.* **1978**, *43*, 3306.
(4) Linn, D. E., Jr.; Rumage, S. D.; Grutsch, J. L., Jr. *Int. J. Chem. Kinet.* **1993**, *25*, 489.
(5) Anast, J. M.; Margerum, D. W. *Inorg. Chem.* **1981**, *20*, 2319.
(6) Berglund, J.; Elding, L. I. In *Laboratory Studies of the Aqueous Chemistry of Free Radicals, Transition Metals and Formation of Acidity in Clouds*; Warneck, P., contract coordinator; Final Report Contract No. STEP-0005-C(MB), April 1, 1990–March 31, 1992; 1992; pp 27–44.
(7) Lim, P. K.; Hamrick, G. T. *J. Phys. Chem.* **1984**, *88*, 1133.
(8) Backström, H. J. *Z. Phys. Chem.* **1934**, *25B*, 122.
(9) Coichev, N.; van Eldik, R. *Inorg. Chem.* **1991**, *30*, 2375.
(10) Coichev, N.; van Eldik, R. *Inorg. Chim. Acta* **1991**, *185*, 69.
(11) Bal Reddy, K.; van Eldik, R. *Atmos. Environ.* **1992**, *26A*, 661.
(12) Berglund, J.; Fronaeus, S.; Elding, L. I. *Inorg. Chem.* **1993**, *32*, 4527.
(13) Huss, A., Jr.; Lim, P. K.; Eckert, C. A. *J. Phys. Chem.* **1982**, *86*, 4229.
(14) Martin, L. R.; Hill, M. W.; Tai, A. F.; Good, T. W. *J. Geophys. Res.* **1991**, *96(D2)*, 3085.
(15) Fuller, E. C.; Crist, R. H. *J. Am. Chem. Soc.* **1941**, *63*, 1644.
(16) Langford, C. H.; Carey, J. H. *Can. J. Chem.* **1975**, *53*, 2430.
(17) Ulrich, P. K.; Rochelle, G. T.; Prada, R. E. *Chem. Eng. Sci.* **1986**, *41*, 2183.
(18) Hobson, D. B.; Richardson, P. J.; Robinson, P. J.; Hewitt, E. A.; Smith, I. *J. Chem. Soc., Faraday Trans. 1* **1986**, *82*, 869.
(19) Lim, P. K.; Huss, A., Jr.; Eckert, C. A. *J. Phys. Chem.* **1982**, *86*, 4233.
(20) Conklin, M. H.; Hoffmann, M. R. *Environ. Sci. Technol.* **1988**, *22*, 883.
(21) Kraft, J.; van Eldik, R. *Inorg. Chem.* **1989**, *28*, 2297.
(22) van Eldik, R. In *Chemistry of Multiphase Atmospheric Systems*; Jaeschke, W., Ed.; NATO ASI Series, Serie G, Springer Verlag: Berlin, Heidelberg, Germany, 1986; Vol. 6, pp 541–566.
(23) Kraft, J. Ph.D. Thesis, University of Frankfurt, Germany 1987.
(24) Danilczuk, E.; Swinarski, A. *Rocz. Chem.* **1961**, *35*, 1563.
(25) Kraft, J.; van Eldik, R. *Inorg. Chem.* **1989**, *28*, 2306.
(26) Waygood, S. J.; McElroy, W. J. *J. Chem. Soc., Faraday Trans.* **1992**, *88*, 1525.
(27) Luňák, S.; Vepřek-Šiška, J. *Collect. Czech. Chem. Commun.* **1976**, *41*, 3495.
(28) Huie, R. E.; Neta, P. *J. Phys. Chem.* **1984**, *88*, 5665.
(29) Deister, U.; Warneck, P. *J. Phys. Chem.* **1990**, *94*, 2191.
(30) Huie, R. E.; Neta, P. *Atmos. Environ.* **1987**, *21*, 1743.

0020-1669/94/1333-0687$04.50/0

as homogeneous catalyst.[13,31] In addition it was unknown how iron(II) was reoxidized into the active iron(III) state, since the spontaneous oxidation with oxygen is very slow in the acidic pH range[33,34] and this is an essential step to complete the catalytic cycle.

However, the question in which way the presence of oxygen could affect both the formation and/or decomposition of the iron(III)–sulfur(IV) complexes and the oxidation state of the metal ion and so accelerate the autoxidation of sulfite remained uncertain in our earlier studies.[21,23,25] Since then more interest has developed in the importance of metal ions and complexes in catalyzed atmospheric oxidation processes.[35-40] This motivated us to further investigate the effect of oxygen on the metal ion catalyzed oxidation of sulfur(IV) oxides, with special emphasis on the redox cycling of the metal ions. Recent studies in our laboratories indicated how sulfite can induce the autoxidation of cobalt(II) and manganese(II) in azide medium[9,10] and of aquated iron(II).[11] The latter results offered a plausible solution of how the catalytic cycle for the iron(III)-catalyzed autoxidation reaction can be completed. It followed that sulfite could play an important role in the redox cycling of iron in atmospheric water.[11] On the basis of this experience, we have now reinvestigated the decomposition of iron(III)–sulfur(IV) complexes in the presence of oxygen in more detail using stopped-flow and oxygen detection techniques. The results reveal direct evidence for the redox cycling of the metal catalyst in the presence of oxygen during the oxidation of sulfite. In this paper we first present a more qualitative description of the kinetics of the decomposition of iron(III)–sulfur(IV) complexes in the presence of oxygen. This is followed by a more quantitative description in which we postulate a kinetic model for the iron(III)-catalyzed oxidation of sulfur(IV) oxides at pH 2.5 which enables us to test the above statements on the autoxidation of sulfur(IV) oxides in the presence of iron(III), and to simulate the overall catalytic cycle and observed kinetic traces.

Experimental Section

Materials. Iron(III) perchlorate (Aldrich), $Fe(ClO_4)_3$, iron(II) perchlorate (Aldrich), $Fe(ClO_4)_2$, and sodium disulfite (Merck), $Na_2S_2O_5$, used in this study were of analytical reagent grade, except for sodium dithionate (97%) (Ferak), $Na_2S_2O_6$, and were used without further purification. Milli-Q-water was used in the preparation of all solutions.

Preparation of Solutions. The iron(III) solutions were prepared freshly every day from a 0.05 M stock solution (pH < 0.2). The sulfur(IV) and iron(II) solutions were prepared freshly for each run. The iron solutions were thermostated at 25 °C in a water bath and then saturated with oxygen. The sulfur(IV) solutions were used as air-saturated solutions in order to avoid any loss in sulfur(IV) concentration by both oxidation and driving out SO_2. The pH of the solutions was adjusted with the aid of $HClO_4$ or NaOH by using a Metrohm or WTW pH-meter with an Ingold pH-electrode. The pH electrode was calibrated with buffers of known pH. Buffers were not used in the kinetic experiments in order to avoid any effects on the reaction. The ionic strength was adjusted with $NaClO_4$.

Instrumentation. A Cary 1 spectrophotometer was used to record spectra and to perform slow kinetic measurements. Rapid-scan spectra were recorded with the aid of an OSMA (Spectroscopy Instruments, Garching, Germany) detector coupled to a Dionex stopped-flow instrument.[41] This setup enabled the recording of spectra at 33-ms time intervals. Fast reactions were followed with a Dionex or Biologic stopped-flow instrument at 390 nm. A fast oxygen detection system (OXYTECH), which is described elsewhere,[42] was used to study the oxygen consumption during the iron(III)-catalyzed sulfur(IV) oxidation. All kinetic measurements were made at an ionic strength of 0.5 M ($NaClO_4$ medium), at pH 2.5 and 25 °C. Rate constants were in general measured under pseudo-first-order conditions. The reported rate constants are mean values of at least 10 individual measurements.

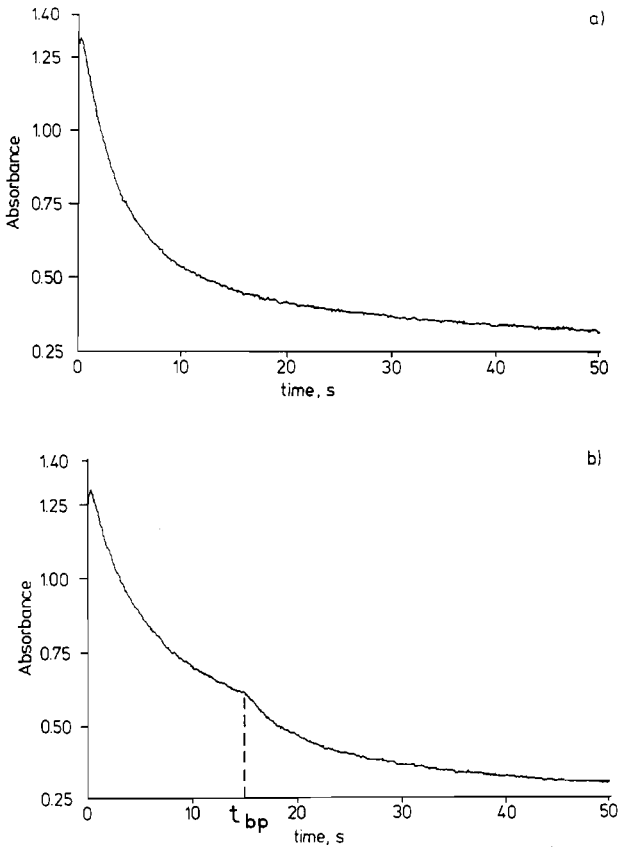

Figure 1. Absorbance–time traces for the iron(III) catalyzed autoxidation of sulfur(IV) oxides: (a) $[O_2] = 0$ M; (b) $[O_2] = 7.5 \times 10^{-4}$ M. Experimental conditions: $[Fe(III)] = 5.0 \times 10^{-4}$ M; $[S(IV)] = 5.0 \times 10^{-3}$ M; ionic strength = 0.5 M; T = 25 °C; pH = 2.5; λ = 390 nm; absorbance scale is in V (10 V = 1 absorbance unit).

Results

Qualitative Observations. When solutions of aquated iron(III) and sulfur(IV) are mixed in the stopped-flow instrument at pH 2.5, the rapid increase in absorbance at 390 nm is followed by a slow decrease due to the redox reaction of the rapidly produced iron(III)–sulfur(IV) complexes when sulfite is used in at least a 10-fold excess. Typical absorbance time traces at 390 nm for argon and oxygen saturated solutions are presented in Figure 1. The trace in Figure 1b clearly shows a peculiar break, almost like a dead end, after which the decay continues further at a faster rate. This break point (at time t_{bp}) is only observed when oxygen is present in the solutions, and its position on the reaction time scale depends on the selected $[O_2]$, [Fe(III)], [Fe(II)], and [S(IV)].[43] A typical set of kinetic traces is reported in Figure

(31) Schlitt, W. J.; Hiskey, J. B.; Pitt, W. G. *Trans. Am. Inst. Min., Metall., Pet. Eng., Soc. Min. Eng. AIME* **1983**, *274*, 2051.
(32) Hoffmann, M. R.; Jacob, D. J. In *SO_2, NO and NO_2 Oxidation Mechanisms*; Calvert, J. G., Ed.; Butterworth Publishers: London, 1984; Vol. 3, pp 101–172.
(33) Luther, G. W. In *Aquatic Chemical Kinetics*; Stumm, W., Ed.; J. Wiley & Sons: New York, 1990; pp 173–198.
(34) Wehrli, B. In *Aquatic Chemical Kinetics*; Stumm, W., Ed.; J. Wiley & Sons: New York, 1990; pp 311–336.
(35) Pandis, S. N.; Seinfeld, J. H. *J. Geophys. Res.* **1989**, *94D*, 1105.
(36) Warneck, P. *Ber. Bunsen-Ges. Phys. Chem.* **1992**, *96*, 454.
(37) Behra, P.; Sigg, L. *Nature* **1990**, *344*, 419.
(38) Zhuang, G.; Yi, Z.; Duce, R. A.; Brown, P. R. *Nature* **1992**, *355*, 537.
(39) Madnawat, P. V. S.; Rani, A.; Sharma, M.; Prasad, D. S. N.; Gupta, K. S. *Atmos. Environ.* **1993**, *27A*, 1985.
(40) Sedlak, D. L.; Hoigné, J. *Atmos. Environ.* **1993**, *27A*, 2173.
(41) Gerhard, A.; Gaede, W.; Neubrand, A.; Zang, V.; van Eldik, R. *Anal. Instrum.*, in press.
(42) Brandt, Ch.; Coichev, N.; Hostert, E.; van Eldik, R. *GIT Fachz. Lab.* **1993**, *37*, 277.
(43) Brandt, Ch.; van Eldik, R. In Photo-oxidants: Precursors and Products. *Proceedings of the Eurotrac Symposium 92, Garmisch-Partenkirchen, Germany, 23rd–27th March 1992*; Borrell, P. M., Borrell, P., Cvitaš, T., Seiler, W., Eds.; SPB Academic Publishing bv: Den Haag, The Netherlands, 1993; pp 593–597.

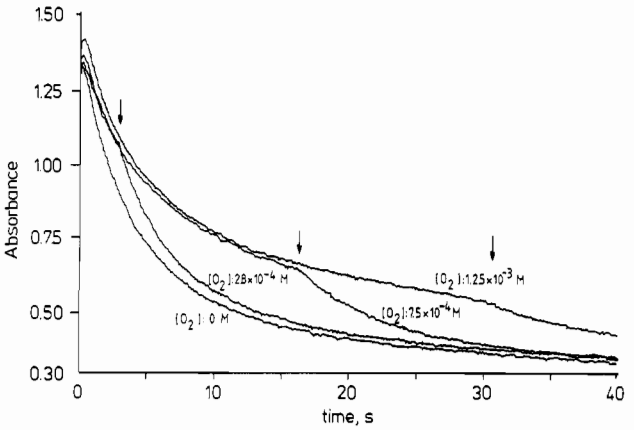

Figure 2. Absorbance–time traces for the iron(III)-catalyzed autoxidation of sulfur(IV) oxides as a function of the $[O_2]$; the arrows indicate t_{bp} in the kinetic traces, i.e. the point where all oxygen is consumed. Experimental conditions: $[Fe(III)] = 5.0 \times 10^{-4}$ M; $[S(IV)] = 5.0 \times 10^{-3}$ M; ionic strength = 0.5 M; $T = 25$ °C; pH = 2.5; $\lambda = 390$ nm, absorbance scale is in V (10 V = 1 absorbance unit).

Table 1. Comparison of t_{bp} Measured with the Stopped-Flow Instrument and the Time of Zero $[O_2]$ Measured with the Oxygen Electrode[a]

[Fe(III)], M	[S(IV)], M	stopped-flow t_{bp}, s	O_2 electrode $t_{[O_2]=0}$, s
1.25×10^{-4}	1.0×10^{-2}	46.7	45.0
2.0×10^{-4}	1.0×10^{-2}	28.9	30.0
2.5×10^{-4}	1.0×10^{-2}	22.5	24.0
5.0×10^{-4}	5.0×10^{-3}	19.4	20.0
6.0×10^{-4}	6.0×10^{-3}	16.0	18.0
1.0×10^{-3}	1.0×10^{-2}	10.4	14.0
1.2×10^{-3}	1.0×10^{-2}	9.1	14.0

[a] $[O_2] = 7.5 \times 10^{-3}$ M; ionic strength = 0.5 M; $T = 25$ °C; pH = 2.5; $\lambda = 390$ nm.

2. In general the break point shows up sooner at lower $[O_2]$, higher [Fe(III)], higher [S(IV)], or lower [Fe(II)]. t_{bp} can usually be determined without any difficulty (unless the time when it occurs becomes too short and it coincides with the formation of the iron(III)–sulfur(IV) complexes) and has been observed within the time range 0.5–120 s, depending on the selected reaction conditions.

A similar series of experiments were performed using a fast oxygen detection system.[42] The typical data in Table 1 clearly demonstrate that the break in the absorbance–time traces occurs at the point where $[O_2]$ is reduced to almost zero. Thus the observed break point results from the termination of a process during which simultaneously oxygen is consumed and the decomposition of the iron(III)–sulfur(IV) species is slowed down. This is interpreted to be due to the sulfite–induced autoxidation of iron(II), which will cause a back-reaction of the produced iron(II) to iron(III) and come to an end exactly at the point where all the oxygen is consumed. Thus the redox cycling of iron as observed elsewhere[11,37,38,40] may be an integrated part of the initial decay of iron(III)–sulfur(IV) complexes and so account for the rather peculiar break point observed in the kinetic traces in the presence of oxygen.

Kinetic Analysis. In this section we will focus on a semiquantitative treatment of the absorbance–time traces and concentrate on the reaction observed in the presence of oxygen. A detailed analysis of the traces in the absence of oxygen as a function of many experimental variables has been performed before.[23] The formation rate of the iron(III)–sulfur(IV) complexes was found to be zero order in oxygen concentration (Table 2), which is in agreement with earlier observations.[21,23] The kinetics of the oxygen induced step are independent of light intensity. Variation of the slit width of the monochromator of the stopped flow instrument in the range of 1 to 2.5 nm had an influence neither

Table 2. Dependence of the Formation Rate Constant k_1 of the Iron(III)-Sulfito Complexes on [S(IV)] and $[O_2]$[a]

10^3[S(IV)], M	k_1, s^{-1}		
	$[O_2] = 0$ M	$[O_2] = 2.6 \times 10^{-4}$ M	$[O_2] = 7.5 \times 10^{-4}$ M
5.0	9.8	9.7	10.8
7.5	13.4	14.7	14.5
10.0	21.5	21.2	21.9
15.0	68.0	69.7	67.1

[a] $[Fe(III)] = 5.0 \times 10^{-4}$ M; ionic strength = 0.5 M; $T = 25$ °C; pH = 2.5; $\lambda = 390$ nm.

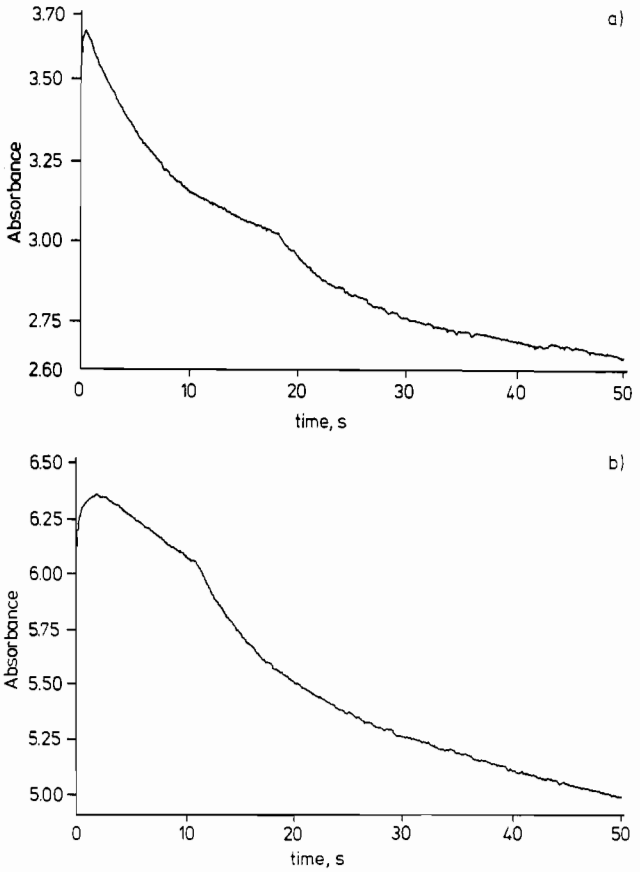

Figure 3. Absorbance–time traces for the iron(III)-catalyzed autoxidation of sulfur(IV) oxides as a function of the initial [Fe(III)] and [S(IV)]: (a) $[Fe(III)] = 5.0 \times 10^{-4}$ M, $[S(IV)] = 5.0 \times 10^{-3}$ M; (b) [Fe(III)] = 1.0×10^{-3} M, $[S(IV)] = 1.0 \times 10^{-2}$ M. Experimental conditions: $[O_2] = 7.5 \times 10^{-4}$ M; ionic strength = 0.5 M; $T = 25$ °C; pH = 2.5; $\lambda = 390$ nm; absorbance scale is in V (10 V = 1 absorbance unit).

on k_{obs} (0.16 ± 0.01 s^{-1}) nor on t_{bp} (19.3 ± 0.6 s; values for the conditions given in Figure 1b).

Two more examples of the oxygen-dependent reaction step are given in Figure 3 to illustrate the different kinetic behavior observed, depending on the selected conditions. The initial absorbance decrease exhibits fairly good first-order behavior (exponential decay) over ca. 75% of the oxygen-induced step (Figures 1 and 3a) at low [Fe(III)], [Fe(II)], and [S(IV)]. Toward the end of this reaction, the decay exhibits a linear behavior and is reminiscent of a typical zero-order process,[44] which is accompanied by the occurrence of a dead end when all the oxygen is consumed (Figure 3a). At high [Fe(III)] and [S(IV)], the oxygen-induced reaction becomes much faster; i.e., the break point in the trace occurs much sooner. At high [Fe(II)] the initial decay reaction is strongly inhibited. Under these conditions (high [Fe(III)], [Fe(II)], and [S(IV)]) only a zero-order decay is observed as can be seen in Figure 3b, and the break point becomes very distinct. It should be noted that rapid scan spectra revealed no

(44) Stochel, G.; van Eldik, R.; Hejmo, E.; Stasicka, Z. *Inorg. Chem.* **1988**, *27*, 2767.

Table 3. Dependence of Extinction Coefficient ϵ on [Fe(III)] and [S(IV)][a]

[Fe(III)], M	[S(IV)], M	ϵ, M^{-1} cm^{-1}
5.0×10^{-4}	5.0×10^{-3}	390
5.0×10^{-4}	1.0×10^{-2}	474
5.0×10^{-4}	2.0×10^{-2}	532
5.0×10^{-4}	2.5×10^{-2}	542
5.0×10^{-4}	3.5×10^{-2}	578
5.0×10^{-4}	4.5×10^{-2}	610
2.0×10^{-4}	1.0×10^{-2}	400
2.5×10^{-4}	1.0×10^{-2}	412
4.0×10^{-4}	1.0×10^{-2}	474
8.0×10^{-4}	1.0×10^{-2}	631
1.0×10^{-3}	1.0×10^{-2}	660
1.5×10^{-3}	1.0×10^{-2}	660

[a] Ionic strength = 0.5 M; pH = 2.5; λ = 390 nm.

evidence for the formation of an intermediate species, which could have accounted for the observed decay behavior as well as the break point phenomenon.

The OLIS KINFIT set of programs[45] was employed to fit the exponential part of the absorbance–time traces. In the case where it was possible, the first- and subsequent zero-order rate constants were separated in a semiquantitative way. The slopes of the linear (zero-order) contribution were converted from –d[absorbance]/dt to –d[Fe^{III}–S^{IV}]/dt by employing the appropriate extinction coefficients (Table 3) of the iron(III)–sulfur(IV) complexes produced under the particular conditions.[21,24]

Influence of Iron(III) and Sulfur(IV) Concentrations. The kinetic results obtained as a function of iron(III) and sulfur(IV) concentrations are summarized in Figures 4–6 (for the effects of iron(II), see the Discussion). On increasing the [Fe(III)], the pseudo-first-order rate constant

$$k_{obs} = -d[Fe^{III}\text{–}S^{IV}]/dt[Fe^{III}\text{–}S^{IV}]$$

exhibits an initial increase and reaches a maximum value at [Fe(III)] $\geq 2 \times 10^{-4}$ M (Figure 4a). The pseudo-zero-order rate constant

$$k_0 = -d[Fe^{III}\text{–}S^{IV}]/dt$$

also increases with increasing [Fe(III)] and tends to reach a maximum value at [Fe(III)] $\geq 6 \times 10^{-4}$ M (Figure 4b). The latter data are subjected to large error limits due to the interference of the initial exponential decay. At [Fe(III)] $> 8 \times 10^{-4}$ M only the pseudo-zero-order reaction (as in Figure 3b) is observed. Similar trends are seen for the influence of [S(IV)] (Figure 5). k_{obs} initially increases with increasing [S(IV)], but soon reaches a limiting value of ca. 0.20 s^{-1} at [S(IV)] $\geq 1 \times 10^{-2}$ M. k_0 exhibits a steady increase with increasing [S(IV)]. On increasing both [Fe(III)] and [S(IV)] at a constant ratio of 1:10, k_{obs} remains fairly constant at 0.15 s^{-1}, whereas k_0 increases slightly with increasing [Fe(III)]/[S(IV)] (Figure 6).

Influence of Iron(II) Concentration. The kinetic traces are strongly affected by the presence of iron(II). It can be clearly seen from Figure 7 that both the formation and decay of the iron(III)–sulfito complexes are significantly slower in the presence of iron(II). The oxygen-induced step observed during the decay of the iron(III)–sulfito complexes is affected by iron(II) in two different ways. The decomposition reaction exhibits a significant increase in t_{bp} at low [Fe(II)] and a clear increase in the importance of the zero-order process at high [Fe(II)] (Figure 7). The values of both k_{obs} and k_0 decrease significantly on increasing the [Fe(II)] (Figure 4a,b), and only the zero-order contribution is observed at [Fe(II)] $> 1 \times 10^{-4}$ M. It should be noted, that the retardation by iron(II) is independent of the oxygen concentration in the solution and is also observed in oxygen-free solutions.

Influence of Oxygen Concentration. We have reported above that the break point in the kinetic traces can be correlated directly with the point where almost all of the dissolved oxygen has been consumed (Table 1). Thus the oxygen detection system should also provide further information on the details of the iron(III)-catalyzed autoxidation of sulfur(IV) oxides. In the absence of

(45) OLIS KINFIT Routines, On-Line Instruments Systems, Inc., Jefferson, GA, 1989.

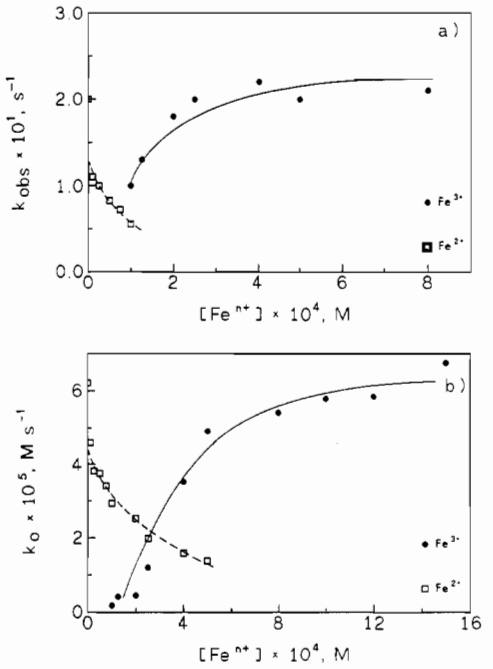

Figure 4. Rate constants as a function of [Fe(III)] and [Fe(II)]: (a) Dependence of first-order rate constant, k_{obs}; (b) Dependence of zero-order rate constant, k_0; experimental conditions: [S(IV)] = 1.0×10^{-2} M; [O_2] = 7.5×10^{-4} M; ionic strength = 0.5 M; T = 25 °C; pH = 2.5; for iron(II) initial [Fe(III)] = 5.0×10^{-4} M.

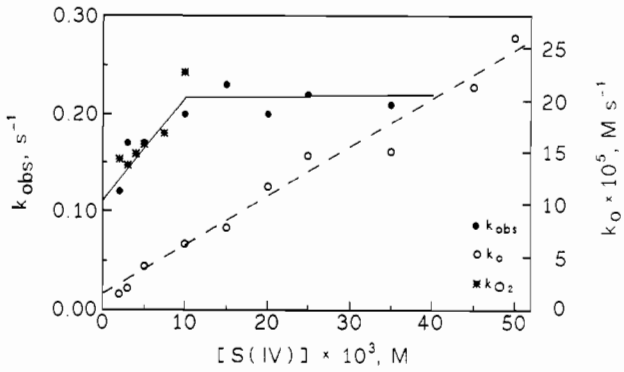

Figure 5. [S(IV)] dependence of the first-order rate constant k_{obs} and the zero-order rate constant k_0, with data for k_{O_2} included (see Discussion). Experimental conditions: [Fe(III)] = 5.0×10^{-4} M; [O_2] = 7.5×10^{-4} M; ionic strength = 0.5 M; T = 25 °C; pH = 2.5.

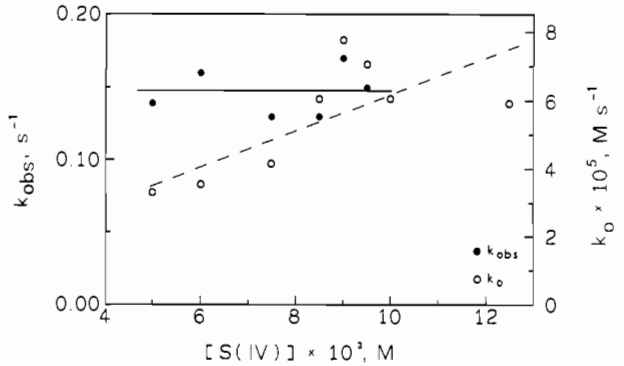

Figure 6. Combined [Fe(III)] and [S(IV)] dependence of the first-order rate constant k_{obs} and the zero-order rate constant k_0 at [Fe(III)]:[S(IV)] = 1:10. Experimental conditions: [O_2] = 7.5×10^{-4} M; ionic strength = 0.5 M; T = 25 °C; pH = 2.5.

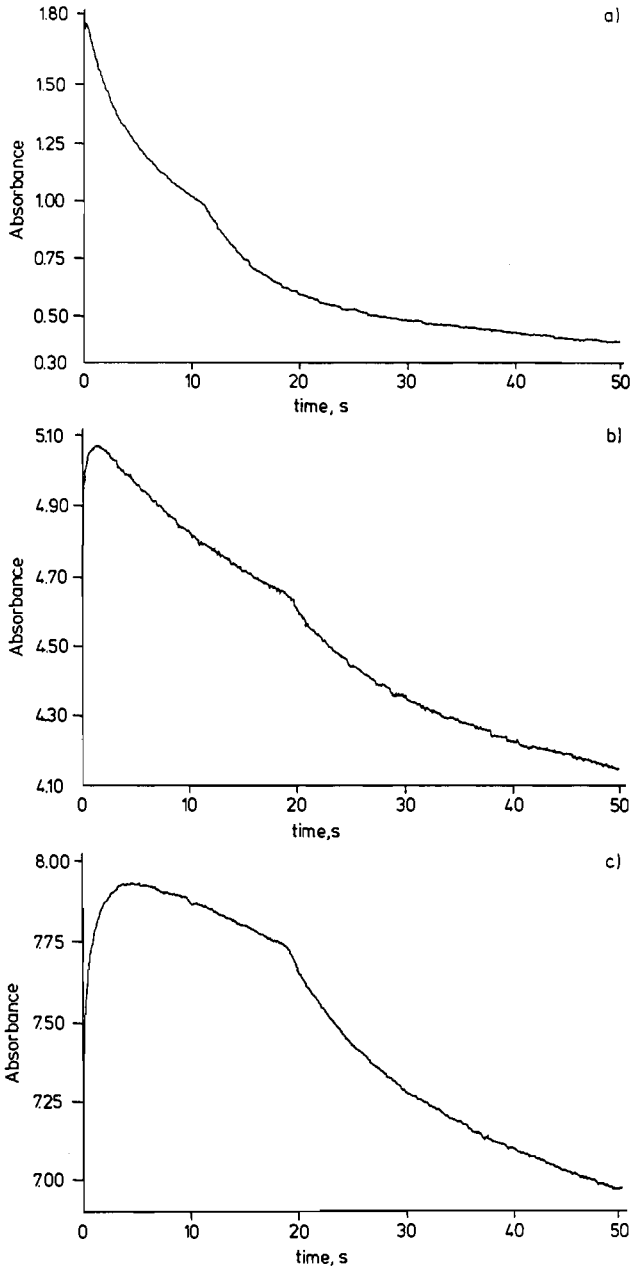

Figure 7. [Fe(II)] dependence of the absorbance–time traces for the iron(III) catalyzed autoxidation of sulfur(IV) oxides: (a) [Fe(II)] = 0 M; (b) [Fe(II)] = 1.0×10^{-4} M; (c) [Fe(II)] = 5.0×10^{-4} M. Experimental conditions: [Fe(III)] = 5.0×10^{-4} M; [S(IV)] = 1.0×10^{-2} M; [O_2] = 7.5×10^{-4} M; ionic strength = 0.5 M; T = 25 °C; pH = 2.5; λ = 390 nm; absorbance scale is in V (10 V = 1 absorbance unit).

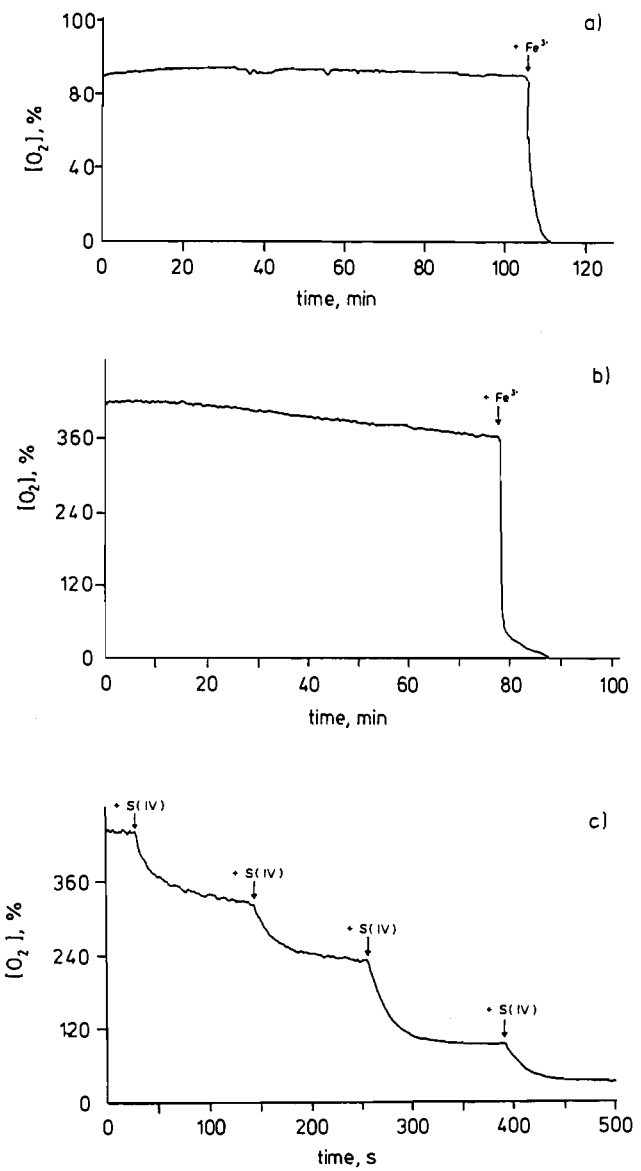

Figure 8. Oxygen consumption during the uncatalyzed and iron(III)-catalyzed autoxidation of sulfur(IV) oxides: (a and b) uncatalyzed autoxidation; (c) iron(III)-catalyzed autoxidation, oxygen saturated solution, with arrows indicating addition of sulfur(IV). Experimental conditions: (a) [S(IV)] = 5.0×10^{-3} M, [O_2] = 2.6×10^{-4} M; ionic strength = 0.5 M; T = 25 °C; pH = 2.5; (b) [S(IV)] = 5.0×10^{-3} M, [O_2] = 1.25×10^{-3} M, ionic strength = 0.5 M, T = 25 °C, pH = 2.5; (c) [Fe(III)] = 5.0×10^{-4} M (V = 20 mL), [S(IV)] = 3.0×10^{-3} M (addition of 1 or 2 mL, respectively), [O_2] = 1.25×10^{-3} M, ionic strength = 0.5 M, T = 25 °C, pH = 2.5.

any added iron(III), oxygen saturated solutions of HSO_3^- at pH 2.5 are practically stable over several hours as indicated in Figure 8a,b. The slight decrease in [O_2] (Figure 8b) is ascribed to the slow loss of oxygen due to diffusion out of the sample chamber of the oxygen detection system. The long time stability of HSO_3^- solutions in the absence of iron(III) exhibited no significant dependence on the initial [O_2] employed, which is in good agreement with that reported in the literature.[46-48] On addition of a small quantity of iron(III) to the HSO_3^- solution, a rapid decrease in the [O_2] occurs due to the catalyzed autoxidation of sulfur(IV) (see Figure 8a,b). If the reaction sequence is changed by starting with an oxygen-saturated solution of iron(III), the addition of a small quantity of sulfite results in the immediate consumption of oxygen, which will depend on the [S(IV)] employed. The results in Figure 8c clearly demonstrate how the oxygen consumption depends on the added [S(IV)], and how the process is initiated by the further addition of sulfite.

In contrast to the usual reaction conditions, the stoichiometric measurements with respect to the consumption of oxygen during the overall redox process were performed where [O_2] $\geq$ [S(IV)]. Thus, the amount of oxygen consumed results in a measurable end concentration of oxygen and can therefore easily be calculated from the difference between initial and final levels. The [O_2] dependence of the iron(III)-catalyzed oxidation reaction reported in Figure 9 shows a linear correlation between the consumed [O_2] and the initial [S(IV)]. The consumed [O_2] is independent of the [Fe(III)] and only slightly dependent of the [Fe(II)] (Figure 10), which demonstrates that only a negligible amount of oxygen

(46) Penkett, S. A.; Jones, B. M. R.; Brice, K. A.; Eggleton, A. E. *Atmos. Environ.* **1979**, *13*, 123.
(47) Larson, T. V.; Horike, N. R.; Harrison, H. *Atmos. Environ.* **1978**, *12*, 1597.
(48) Bhargava, R.; Prasad, D. S. N.; Rani, A.; Bhargava, P.; Jain, U.; Gupta, K. S. *Transition Met. Chem. (Weinheim, Ger.)* **1992**, *17*, 238.

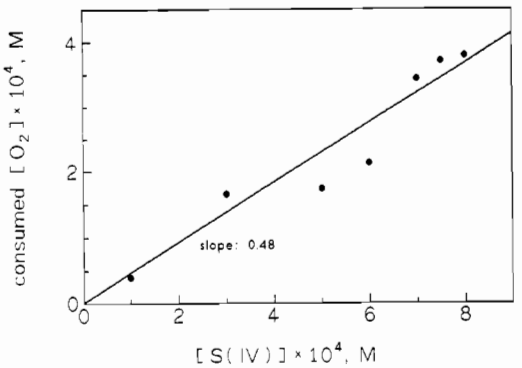

Figure 9. Oxygen consumption as function of [S(IV)]. Experimental conditions: [Fe(III)] = 5.0×10^{-4} M; $[O_2] = 7.5 \times 10^{-4}$ M; ionic strength = 0.5 M; T = 25 °C; pH = 2.5.

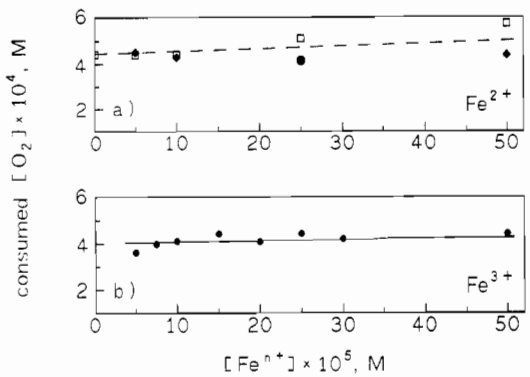

Figure 10. Oxygen consumption as function of (a) [Fe(II)] and (b) [Fe(III)]. Experimental conditions: [S(IV)] = 7.5×10^{-4} M; $[O_2] = 7.5 \times 10^{-4}$ M; ionic strength = 0.5 M; T = 25 °C; pH = 2.5; for iron(II), initial [Fe(III)] = 5.0×10^{-4} M (open squares) and $[Fe^{n+}] = 5.0 \times 10^{-4}$ M (closed rhombs), respectively.

is used for the oxidation of iron(II) or the redox cycling of iron(II/III). Furthermore, the results in Figure 10b reveal no evidence for the formation of any oxygen-coordinated sulfite complexes as suggested in the literature.[1,25,49,50]

A number of experiments were performed in which the time dependence of the $[O_2]$ was used to obtain kinetic data for the oxygen consumption. Kinetic traces recorded with the oxygen electrode indicated a fairly good exponential behavior over the first 3 half-lives of the reaction (Figure 11), that is up to the point where 87% of the available oxygen has been consumed. Deviations from the exponential behavior at longer reaction times are most probably due to slow diffusion processes within the membrane section of the electrode[42] that affect the time resolution of the instrument at low concentrations. The first 3–5 s were not included in the calculations in order to avoid any interference of the mixing process. The observed first-order rate constants, k_{O_2}, exhibit characteristic dependences on both the [Fe(III)] and [Fe(II)] as illustrated in Figure 12a. The value of k_{O_2} increases with increasing [Fe(III)] and reaches a limiting value at [Fe(III)] > 2×10^{-4} M, whereas it is not affected by [Fe(II)]. In fact the [Fe(III)] dependence is in close agreement with that observed spectrophotometrically (see Figure 4a), but the [Fe(II)] dependence differs totally. The [S(IV)] dependence of k_{O_2} could only be studied over a limited concentration range, and the results indicate an increase in k_{O_2} with increasing [S(IV)] as shown in Figure 12b. A comparison of these data with those found spectrophotometrically (Figure 5) indicate that the values of k_{O_2} are exactly a factor 2 smaller than the values of k_{obs} found under these conditions. This is presumably related to the linear

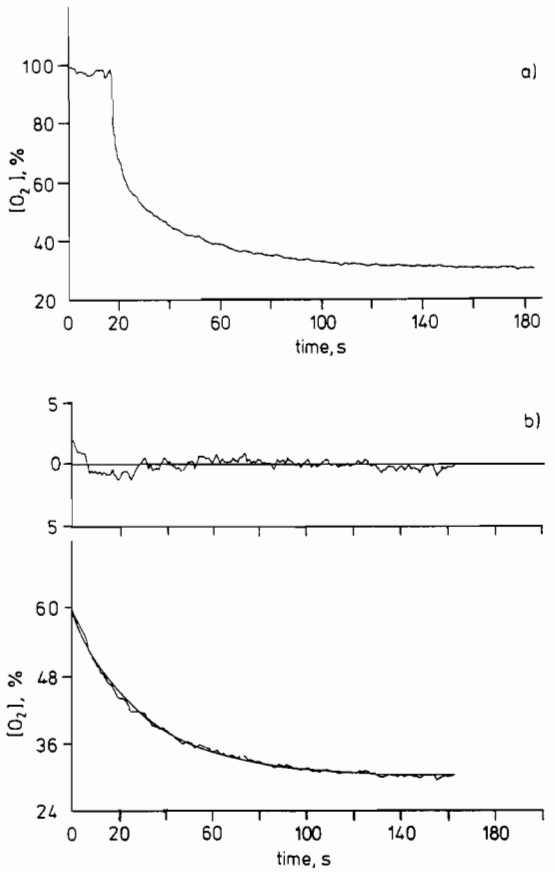

Figure 11. Oxygen–time trace for the iron(III)-catalyzed autoxidation of sulfur(IV) oxides. Experimental conditions: (a) [Fe(III)] = 5.0×10^{-4} M, [S(IV)] = 7.0×10^{-4} M, $[O_2] = 7.5 \times 10^{-4}$ M, ionic strength = 0.5 M, T = 25 °C, pH = 2.5; (b) first-order fit of trace in part a.

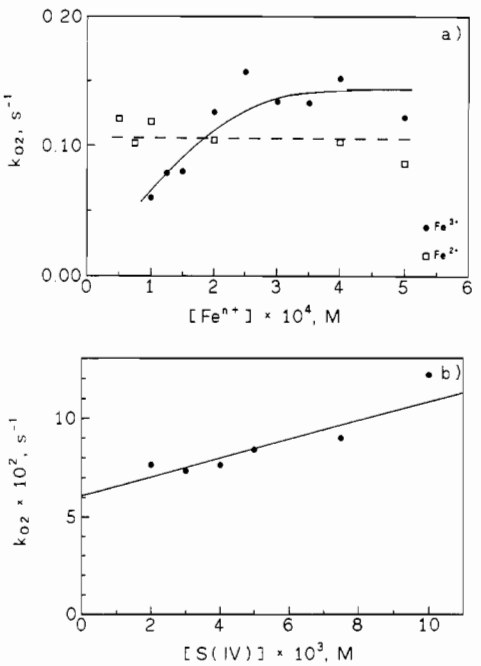

Figure 12. k_{O_2} as function of (a) $[Fe^{n+}]$ and (b) [S(IV)]: (a) [S(IV)] = 1.0×10^{-2} M, (for iron(II), initial [Fe(III)] = 5.0×10^{-4} M); (b) [Fe(III)] = 5.0×10^{-4} M. Experimental conditions: $[O_2] = 7.5 \times 10^{-4}$ M; ionic strength = 0.5 M; T = 25 °C, pH = 2.5.

dependence between the consumed $[O_2]$ and the initial [S(IV)] (slope 0.48) as demonstrated by the data in Figure 9. Inclusion of the $2k_{O_2}$ data in Figure 5 illustrates the good agreement between the spectrophotometrically and potentiometrically obtained kinetic data.

(49) Boyce, S. D.; Hoffmann, M. R.; Hong, P. A.; Moberly, L. M. *Environ. Sci. Technol.* **1983**, *17*, 602.
(50) Pasiuk-Bronikowska, W.; Bronikowski, T. *Chem. Eng. Sci.* **1989**, *44*, 1361.

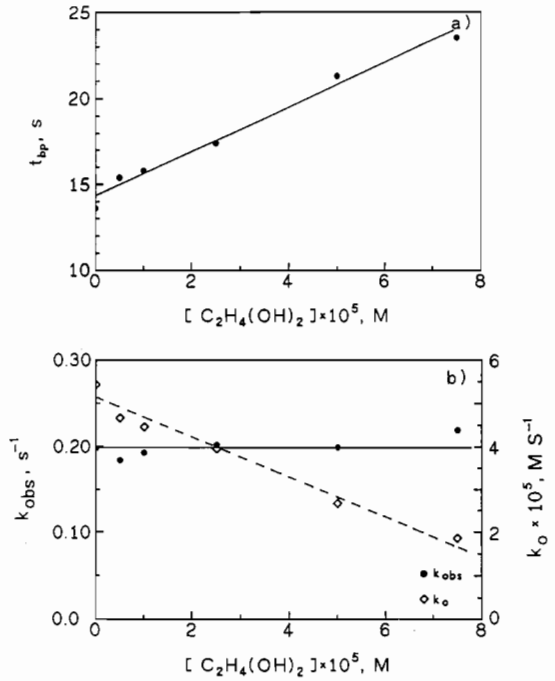

Figure 13. Effect of hydroquinone on (a) t_{bp}, and (b) k_{obs} and k_0. Experimental conditions: [Fe(III)] = 5.0×10^{-4} M; [S(IV)] = 5.0×10^{-3} M; [O_2] = 7.5×10^{-4} M; ionic strength = 0.5 M; T = 25 °C; pH = 2.5.

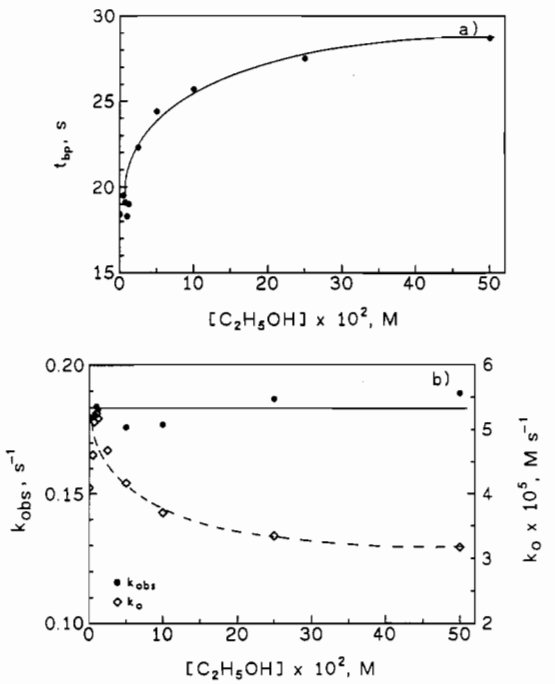

Figure 14. Effect of ethanol on (a) t_{bp}, and (b) k_{obs} and k_0. Experimental conditions: [Fe(III)] = 5.0×10^{-4} M; [S(IV)] = 5.0×10^{-3} M; [O_2] = 7.5×10^{-4} M; ionic strength = 0.5 M; T = 25 °C; pH = 2.5.

Effect of Radical Scavengers. The effects of different radical scavengers on the oxygen induced step during the iron(III)-catalyzed oxidation of sulfur(IV) oxides are summarized in Figures 13 and 14. Under the selected experimental conditions hydroquinone is a much stronger reaction inhibitor than ethanol. Both radical scavengers show no effect on the decomposition rate of the iron(III)–sulfito complexes in Ar-saturated solutions. In the presence of oxygen, t_{bp} increases linearly with increasing hydroquinone concentration. With increasing ethanol concentration, t_{bp} reaches a limiting value at [C_2H_5OH] ≥ 0.2 M. In the case of ethanol no inhibition of the decomposition of the iron(III)–sulfito complexes in the presence of oxygen was observed up to [C_2H_5OH] ≤ 1.25×10^{-2} M. By way of comparison, the presence of [$C_6H_4(OH)_2$] ≥ 5×10^{-6} M results in a certain inhibition under the selected reaction conditions.

Both radical scavengers used in this work show the same effect on the exponential and the linear decay. k_{obs} is not affected by varying the concentration of the radical scavengers within the experimental error. In the case of hydroquinone, k_0 decreases linearly with increasing concentration, whereas k_0 reaches a limiting value at [C_2H_5OH] ≥ 0.2 M. An increase in [C_2H_5OH] from 0 to 0.5 M has no influence on the solubility of oxygen ([O_2] = (2.4–2.5) × 10^{-4} M at 25 °C). No dependence of the consumed oxygen on [$C_6H_4(OH)_2$] was observed within the experimental error limits. For the conditions given for Figure 1b the amount of oxygen consumed is (2.62 ± 0.05) × 10^{-4} M for 0 ≤ [$C_6H_4(OH)_2$] ≤ 1.0×10^{-4} M.

Qualitative Mechanistic Interpretation. As outlined above, it is our objective to first discuss the results of the present study in a more qualitative way using a simplified reaction scheme in order to highlight some important mechanistic features.

The catalytic effect of light on the autoxidation of dissolved sulfite is known.[27,51,52] Luňák and Vepřek-Šiška[27] show that the photoinitiated autoxidation of sulfite is catalyzed by iron(III). They suggest that the photochemical autoxidation of sulfite is not initiated via absorption of light by a free sulfite anion but by its iron(III)–sulfito complex. The results of changing the slit width of the monochromator of the stopped flow instrument clearly indicate that light has no influence on either the reaction rate or the oxygen consumption under the selected reaction conditions. Thus, the observed oxygen-induced step is only due to the presence of oxygen in the solution.

The [Fe(III)] and [S(IV)] dependencies of k_{obs} and k_0 reported in Figures 4–6 reveal important qualitative information on the nature of the observed reaction steps. The observed kinetic traces indicate that the presence of oxygen in general slows down the redox decomposition of the iron(III)–sulfito complexes. This can only be due to the sulfite-induced autoxidation of the produced iron(II) to iron(III),[11] which will cause a reproduction of iron(III), as can be clearly seen from the traces in Figure 2. Thus the initial first-order decay can be related to the redox behavior of the iron(III)–sulfito complexes, whereas the subsequent zero-order behavior with the associated break point must be mainly due to the back-reaction that becomes important under such conditions. The gradual changeover from an exponential (first-order) to a linear (zero-order) decay in the presence of oxygen may be due to the attainment of steady state conditions, where –d[Fe(III)–S(IV)]/dt reaches a constant value, i.e. a decay independent of the [Fe(III)–S(IV)]. Figure 7 supports this trend in that the linear part of the decay curve becomes increasingly prominent on increasing the [Fe(II)], i.e. on increasing the importance of the back-reaction.

The catalytic effect of iron(III) on the autoxidation of sulfur(IV) reaches a maximum value at 2×10^{-4} M iron(III), whereas the [S(IV)] controls the nature of the complex being formed.[21,24] The maximum k_{obs} value of ca. 0.20 s^{-1} is slightly higher than the value of 0.15 s^{-1} reported before,[25] although this may be due to the significantly higher ionic strength (0.5 M) selected in the present study, compared to 0.1 M before (see further Discussion). The values of k_0 increase significantly with increasing [Fe(III)] and [S(IV)] concentrations, which indicates that the reverse oxidation of iron(II) to iron(III) strongly depends on the production of $SO_3^{\bullet-}$ radicals, since these are formed during the decomposition of iron(III)–sulfito complexes. Again the [Fe(III)] effect on k_0 will reach a saturation when the production of $SO_3^{\bullet-}$ radicals is not rate-limiting anymore. At this stage a qualitative scheme that can account for the observed trends can be summarized as given in Scheme 1. These reactions are followed

(51) Dogliotti, L.; Hayon, E. *J. Phys. Chem.* **1967**, *72*, 1800.
(52) Frank, S. N.; Bard, A. J. *J. Geophys. Chem.* **1977**, *81*, 1484.

Scheme 1

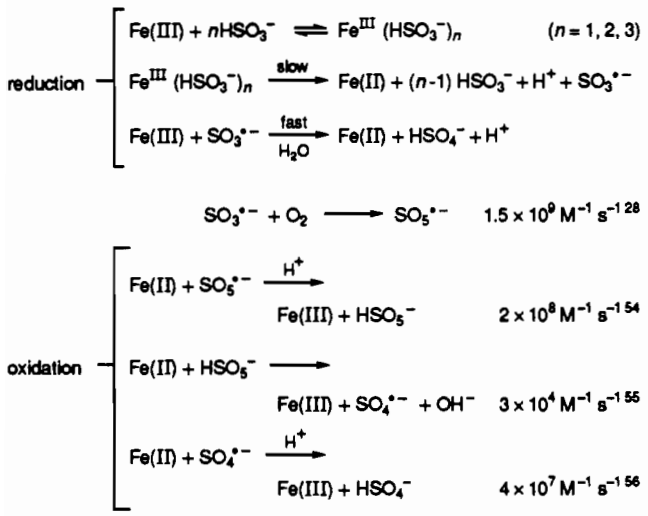

by a series of free radical propagation, termination, and product formation reactions that result in the overall oxidation of sulfite to sulfate. Details on these are given elsewhere[9,11,36,53] and in the Discussion.

The first reactions in Scheme 1 represent the reduction of the iron(III)–sulfito complexes, which is controlled by the nature of the complex produced under the selected experimental conditions.[25] The $SO_3^{\bullet-}$ radical can subsequently either reduce a further iron(III) species, oxidize iron(II) to iron(III), or dimerize to produce $S_2O_6^{2-}$. The latter two possibilities can account for the deviation from strictly exponential behavior of the decay process at longer reaction times, i.e. after 2 half-lives. For the importance of these individual contributions see the further Discussion. In the presence of oxygen, $SO_3^{\bullet-}$ rapidly produce $SO_5^{\bullet-}$, which is generally accepted to be a strong oxidant ($E(SO_5^-/HSO_5^-) = 1.1$ V, pH 7)[28] and can in a series of reactions oxidize iron(II) to iron(III). Thus, in the presence of oxygen, the formation of $SO_5^{\bullet-}$ will compete with the reduction of iron(III) by $SO_3^{\bullet-}$. At the point where the oxygen is used up, no $SO_5^{\bullet-}$ can be produced and oxidation of iron(II) to iron(III) comes to an end. This causes a break point in the absorbance–time traces, followed by the further decomposition of the remaining iron(III)–sulfito species. The oxidation of iron(II) to iron(III) exhibits a zero-order behavior which accounts for the linear parts of the absorbance–time plots close to the jump itself since this is a characteristic for zero-order reactions.[44] Free radical reactions not included in Scheme 1 are those of $SO_5^{\bullet-}$ and $SO_4^{\bullet-}$ with HSO_3^- to produce $SO_3^{\bullet-}$, HSO_5^-, and SO_4^{2-}, respectively. These are important competitors for the oxidation of iron(II), especially at low [Fe(II)] and high [S(IV)], and form an important aspect of the overall mechanism (see further Discussion).

A retarding effect of iron(II) on the rate of the iron(III)-catalyzed sulfur(IV) oxidation has been observed earlier,[57–59] whereas Carlyle[60] found no influence of iron(II) on the formation rate of the iron(III)–sulfito complexes. The inhibition by iron(II) of the decomposition of the iron(III)–ascorbate complex has been reported.[61] Furthermore, a catalytic effect of iron(II) on the aquation of nitropentacyanoferrate(III) has been reported.[44] In both the manganese(III)- and the copper(III)-catalyzed oxidation of sulfur(IV) oxides, the addition of manganese(II) or copper(II), respectively, resulted in a decrease in the reaction rate.[5,62]

The inhibition of the decomposition of the iron(III)–ascorbate complex by iron(II)[61] was explained in terms of an equilibration between the iron(III)–ascorbate complex and iron(II). Due to the much lower stability of the iron(III)–ascorbate complex ($K \sim 2$ M^{-1})[63] in comparison to the iron(III)–sulfito complexes ($K = 600$ M^{-1}),[21] the suggested mechanism for the iron(III)–ascorbate system seems to be unlikely for the iron(III)–sulfur(IV) system. It was reported that iron(II) acts as a scavenger for the $SO_3^{\bullet-}$ radical.[27] The rate constant (9.8×10^6 M^{-1} s^{-1})[64] is significantly lower than that for the formation of the $SO_5^{\bullet-}$ radical ($(1.2–2.5) \times 10^9$ M^{-1} s^{-1}),[28,29,64] such that under the selected conditions ([Fe(III)] < [S(IV)]), this reactions may have a small effect on the rate of formation and decomposition of the iron(III)–sulfito complexes (see Discussion).

In a qualitative way the decrease in k_{obs} with increasing [Fe(II)] must be due to the increased rate of production of iron(III), thus a slower overall decomposition of the iron(III)–sulfito complexes. In a similar way, a more efficient oxidation to iron(III) at higher [Fe(II)] will offset the decomposition reaction and force the system to approach an equilibrium situation, i.e. a slower reaction rate (k_0), as seen in Figures 4b and 7c. According to the suggested mechanism in Scheme 1, the exponential part of the decay process must result in a k_{obs} at least twice as large in the absence of oxygen than in its presence under conditions where the back-reaction operates effectively. The results in Figure 4a clearly show the drastic decrease in k_{obs} on increasing [Fe(II)] in the presence of oxygen. It should therefore be possible, under certain conditions, to observe an increase or a constant absorbance in the kinetic traces when the formation rate of iron(III)–sulfito complexes is larger than or equal to the rate of decay, respectively. Such an increase in absorption has been observed for the sulfite-induced oxidation of iron(II)[65] and manganese(II).[10] In both cases the metal ion was present in large excess compared to [S(IV)]. Furthermore, the balance between the reduction and oxidation steps in Scheme 1 will also be controlled by the $[O_2]$ employed. Measurements of the oxygen consumption (Figure 9) demonstrate a linear dependence between the $[O_2]$ consumed and the initial [S(IV)] employed (ratio 1:2), and a slight increase in the consumption of oxygen with increasing [Fe(II)] (Figure 10). The results clearly indicate that oxygen is mainly consumed during the overall oxidation of sulfite to sulfate (eq 1) and that

$$HSO_3^- + {}^1/_2O_2 \xrightarrow{Fe^{3+}} SO_4^{2-} + H^+ \qquad (1)$$

very little is really used for the autoxidation of iron(II) to iron(III) under the selected reaction conditions ($[S(IV)] \gg [O_2]$). The stoichiometry in eq 1 is in line with other results on the transition-metal catalyzed oxidation of sulfur(IV) oxides[66,67] and is in good agreement with the suggested mechanism in which iron(II) is only oxidized indirectly via sulfur oxide radicals. According to the suggested mechanism in Scheme 1, [Fe(II)] should not affect the overall rate of oxygen consumption (Figure

(53) Hoffmann, M. R.; Calvert, J. G. *Chemical Transformation Modules for Eulerian Acid Deposition Models, Vol. II. The Aqueous Phase Chemistry* EPA-600/3-85/017; GPO: Washington, DC, 1985.
(54) Waygood, S. J. Poster presented at the Eurtotrac Meeting, March 23–27, 1992, Garmisch-Partenkirchen, Germany.
(55) Gilbert, B. C.; Stell, J. K. *J. Chem. Soc., Perkin Trans.* **1990**, *2*, 1281.
(56) McElroy, W. J.; Waygood, S. J. *J. Chem. Soc., Faraday Trans.* **1990**, *86*, 2557.
(57) Burriel-Marti, F.; Lucena Conde, F. *Anal. Chim. Acta* **1949**, *3*, 547.
(58) Higginson, W. C. E.; Marshall, J. W. *J. Chem. Soc.* **1957**, 447.
(59) Zeck, O. F.; Carlyle, D. W. *Inorg. Chem.* **1974**, *13*, 34.
(60) Carlyle, D. W. *Inorg. Chem.* **1971**, *10*, 761.
(61) Xu, J.; Jordan, R. B. *Inorg. Chem.* **1990**, *29*, 4180.
(62) Siskos, P. A.; Peterson, N. C.; Huie, R. E. *Inorg. Chem.* **1984**, *23*, 1134.
(63) Bänsch, B.; Martinez, P.; Uribe, D.; Zuluaga, J.; van Eldik, R. *Inorg. Chem.* **1991**, *30*, 4555.
(64) Buxton, G. V.; Croft, S.; McGowan, S. In *Laboratory Study of the Aqueous Chemistry of Free Radicals, Transition Metals and Formation of Acidity in Clouds*; Warneck, P., contract coordinator; Final Report Contract No. STEP-0005-C(MB); April 1, 1990–March 31, 1992; 1992; pp 61–74.
(65) Bal Reddy, K.; Coichev, N.; van Eldik, R. *J. Chem. Soc., Chem. Commun.* **1991**, 7, 481.
(66) Faust, B. C.; Hoffmann, M. R.; Bahnemann, D. W. *J. Phys. Chem.* **1989**, *93*, 6371.
(67) Brandt, Ch.; van Eldik, R. Unpublished results.

12a); it should however affect the rate of iron(III) formation and cause the overall decrease in [Fe(III)] to slow down as indicated in Figure 4a.

The changeover from an exponential (first-order) to a linear (zero-order) decay in the presence of oxygen has been demonstrated to result from an increase in [Fe(III)], [Fe(II)], or [S(IV)], while the others are held constant. Interestingly, an increase in [Fe(III)] and [S(IV)] in the constant ratio of 1:10 also results in the changeover (Figure 6), indicating that the ratio [Fe(III), Fe(II), S(IV)]:[O_2] is an important factor during the overall decay of the iron(III)–sulfito complexes. k_{obs} remains nearly unaffected whereas k_0 increases slightly. Because of the constant ratio [Fe(III)]:[S(IV)] = 1:10, no change in k_{obs} is expected since k_{obs} represents the decay of the iron(III)–sulfito complexes. High [Fe(III)] and high [S(IV)] result in a higher formation rate of the sulfite radical anion $SO_3^{\bullet-}$, and the reoxidation of iron(II) becomes more important and k_0 increases.

Quantitative Treatment of Data. A more quantitative treatment of the suggested mechanism in Scheme 1 must include a kinetic balance between the reduction and reoxidation reactions of the iron(III)–sulfito complexes as expressed in (2) in which k_{red} and

$$-d[Fe^{III}\text{–}S^{IV}]/dt = (rate)_{reduction} - (rate)_{oxidation} = k_{red}\{[Fe(III)], [S(IV)]\} - k_{ox}\{[Fe(II)], [SO_3^{\bullet-}], [O_2]\} \quad (2)$$

k_{ox} represent overall rate constants for the reduction and oxidation steps, respectively. Under conditions where [Fe(II)] and [O_2] are low, the contribution of the oxidation steps will be negligible and k_{red} will be close to that found before for the reduction of the iron(III)–sulfito species in the absence of oxygen.[35] When [Fe(II)] is increased in the presence of oxygen, the contribution of the reverse oxidation process increases to such an extent that $-d[Fe^{III}\text{–}S^{IV}]/dt$ reaches a constant value, i.e. the reaction rate becomes apparently independent of [Fe^{III}–S^{IV}], and the overall reaction exhibits zero-order character (k_0 data in Figures 4–6). The sulfite-induced autoxidation of iron(II) was studied in more detail before,[11,65] but under conditions where iron(II) was always in a large excess compared to iron(III). A quantitative fit of the kinetic data of k_0 in Figures 4b and 5 is complicated by the fact that the concentration of iron(II), which causes the reoxidation reaction and the occurrence of zero-order kinetics, is unknown.

The rate of reduction of iron(III) by sulfur(IV) oxides can be expressed as k_{red}[Fe(III)][S(IV)] in the presence of oxygen, for which k_{red} = 28.2[25] and 30[11] M^{-1} s^{-1} at 25 °C and 0.1 M ionic strength. Similar experiments were repeated in this study at 0.5 M ionic strength, and k_{red} was found to have the value 15.2 M^{-1} s^{-1}. The rate of oxidation of iron(II) can be expressed as k_{ox}\{[Fe(III)] + [S(IV)]\},[11] where k_{ox} = 320 M^{-1} s^{-1} at pH = 3.1 and 0.1 M ionic strength, and k_{ox} = 160 M^{-1} s^{-1} at pH = 2.5. A systematic study of ionic strength dependence[67] indicated that this value reduces further to 133 M^{-1} s^{-1} at pH 2.5 and 0.5 M ionic strength. Thus under the conditions selected in this study, these rate data can be substituted in eq 2 and result in the overall expression (3). A semiquantitative fit of the [Fe(II)] dependence

$$-d[Fe^{III}\text{–}S^{IV}]/dt = 15.2[Fe(III)][S(IV)] - 133[S(IV)][Fe(II)] \quad (3)$$

of k_0 in Figure 4b, for which [Fe(III)] = 5×10^{-4} M and [S(IV)] = 1×10^{-2} M, with the aid of eq 3 resulted in k_{red} and k_{ox} values of 12.4 and 90 M^{-1} s^{-1}, respectively. This demonstrates that the results of the present investigation are in good agreement with those reported before.[11,25]

The [Fe(III)] and [S(IV)] dependencies (k_0) reported in Figures 4b and 5 can for a limited concentration range be expressed as $k_0 = 7.5$[Fe(III)][S(IV)] and $k_0 = 11$[Fe(III)][S(IV)] M s^{-1}, respectively. These overall values are smaller than the first term in eq 3 and must include a negative contribution from the k_{ox}[S(IV)][Fe(II)] term. In fact a 5% conversion of iron(III) to iron(II) will be enough to account for the mentioned difference. Thus relatively low iron(II) concentrations are required to cause an effective reoxidation to iron(III) which is induced by sulfite. The first (reduction) term in eq 3 can be accounted for by the first three reactions given in Scheme 1. The second (oxidation) term in eq 3 requires some preequilibrium steps with iron(II) to account for the saturation effect observed in Figure 4b. This could for instance be the reactions outlined in (4) or similar steps

$$Fe(II) + SO_5^{\bullet-} \rightleftharpoons Fe^{II}\text{–}SO_5^- \qquad Fe^{II}\text{–}SO_5^- \xrightarrow{H^+} Fe(III) + HSO_5^- \quad (4)$$

involving the interaction of HSO_5^- and $SO_4^{\bullet-}$ with iron(II) to simultaneously oxidize iron(II) to iron(III) and sulfite to sulfate. Evidence for such a saturation effect at high [Fe(II)] was not observed before.[11]

Variations in the [O_2] have a remarkable effect on the observed kinetic traces, in that the value of t_{bp} increases with increasing dissolved [O_2]. This is quite understandable since the higher [O_2] will allow the redox cycling of iron(II/III) to continue for a longer time until the oxygen is consumed. Thus an increase in [O_2] significantly slows down the overall decomposition of the iron(III)–sulfur(IV) species, which in terms of the suggested mechanism in Scheme 1, is due to a more effective redox cycling and oxidation of iron(II) to iron(III) under such conditions.

The k_{obs} values represent the decay of the iron(III)–sulfito complexes, which result in the formation of $SO_3^{\bullet-}$ radicals. The stoichiometric measurements of this study indicate that the reaction of oxygen with the $SO_3^{\bullet-}$ radical is the most important oxygen-consuming process during the overall redox reaction. Due to the very fast formation of the $SO_5^{\bullet-}$ radical (see Scheme 1), the formation of the $SO_3^{\bullet-}$ radical is the rate-determining step in the consumption of oxygen. The concentration range where both k_{obs} and k_{O_2} are independent of the initial [Fe(III)] is ascribed to the nature of the iron(III)–sulfito complexes present under such conditions.[21] For a particular iron(III)–sulfur(IV) ratio only a specific type of iron(III)–sulfito complex will be formed.[21,24]

The retarding effect of some substances on the sulfur(IV)-oxidation process (negative catalysis) has been known for a long time and was first studied in a systematic way by Bigelow[68] in 1898. In particular, chelating agents and phenolic antioxidants seem to have a certain inhibiting effect in the case of the sulfur(IV) oxidation process.[19] It is assumed that the inhibiting effect of these substances is due to their ability to react rapidly with the radicals produced during the oxidation reaction (Table 4). Some radical scavengers react only with selected radicals in an efficient way. Ethanol for example reacts with both $OH^{\bullet}$ and $SO_4^{\bullet-}$ radicals,[29] but $SO_3^{\bullet-}$ and $SO_5^{\bullet-}$ are relatively inert to ethanol.[69] In the absence of oxygen (Ar-saturated solutions) no influence of ethanol and hydroquinone on the decomposition rate of the iron(III)–sulfito complexes is observed (Figures 13 and 14). In terms of the suggested mechanism (Scheme 1) in the absence of oxygen, $SO_3^{\bullet-}$ radicals are produced during the decomposition reaction. As mentioned above, ethanol should not react with the

(68) Bigelow, S. L. *Z. Phys. Chem.* **1898**, *28*, 493.
(69) Hayon, E.; Treinin, A.; Wilf, J. *J. Am. Chem. Soc.* **1972**, *94*, 47.
(70) Huie, R. E.; Neta, P. *J. Phys. Chem.* **1986**, *90*, 1193.
(71) Huie, R. E.; Neta, P. *J. Phys. Chem.* **1985**, *89*, 3918.
(72) Eibenberger, H.; Steenken, S.; O'Neill, P.; Schulte-Frohlinde, D. *J. Phys. Chem.* **1978**, *82*, 749.
(73) Heckel, E.; Henglein, A.; Beck, G. *Ber. Bunsen-Ges. Phys. Chem.* **1966**, *70*, 149.
(74) Dogliotti, L.; Hayon, E. *J. Phys. Chem.* **1967**, *71*, 2511.
(75) Kraljić, I. *Int. J. Radiat. Phys. Chem.* **1970**, *2*, 59.
(76) Neta, P.; Huie, R. E. *Environ. Health Perspect.* **1985**, *64*, 209.

Table 4. Rate Constants for the Reaction of $SO_3^{\bullet-}$, $SO_4^{\bullet-}$, and $SO_5^{\bullet-}$ with Ethanol and Hydroquinone

reaction	k, M^{-1} s^{-1}	pH	ref
$SO_3^{\bullet-} + C_2H_5OH$	$\leq 2.0 \times 10^3$		69
$SO_3^{\bullet-} + C_6H_4(OH)_2$	4.5×10^6	8.9	70
	1.0×10^7	9.0	71
	5.4×10^7	10.5	70
	1.2×10^8	11.2	71
	3.2×10^8	13.0	71
$SO_4^{\bullet-} + C_2H_5OH$	1.6×10^7	7–8	72
	3.0×10^7	1.0	73
	6.2×10^7	1.0	74
	6.2×10^7	9.0	75
	7.7×10^7	4.8	74
$SO_4^{\bullet-} + C_6H_4(OH)_2$	$\geq 10^9$ [a]		76
$SO_5^{\bullet-} + C_2H_5OH$	$\leq 10^3$	9.0	69
$SO_5^{\bullet-} + C_6H_4(OH)_2$	2.7×10^6	6.6	71
	2.0×10^7	9.5	71

[a] Estimated value.

$SO_3^{\bullet-}$ radical in a rate-determining way. In the case of hydroquinone, a reaction between the sulfite radical and hydroquinone has been proposed in order to explain the inhibiting effect of the latter compound on the oxidation of sulfur(IV) oxides.[19] However, the reaction was studied in the presence of oxygen, such that $SO_5^{\bullet-}$ and HSO_5^- are formed during the redox process, which may have reacted with hydroquinone instead of $SO_3^{\bullet-}$.

We have separated the kinetics of the oxygen induced step during the decomposition of the iron(III)–sulfito complexes into an exponential and a linear decay part. It is suggested, in our simplified mechanistic model (Scheme 1) that the exponential decay is due to the decomposition of the iron(III)–sulfito complexes during which $SO_3^{\bullet-}$ radicals are produced. This step is similar to the decomposition in the absence of any oxygen. The reoxidation of iron(II) back to iron(III) with the formation of new iron(III)–sulfito complexes ([S(IV)] $\gg$ [Fe(III)]) causes the linear part in the absorbance time trace. The use of radical scavengers proves this suggestion. As mentioned above, ethanol and hydroquinone do not react with $SO_3^{\bullet-}$ with an observable influence under the selected reaction conditions. Thus the exponential decay, described by k_{obs}, should not be affected by the presence of ethanol or hydroquinone. This is in agreement with the data in Figures 13 and 14. If ethanol and hydroquinone react with $SO_5^{\bullet-}$ and/or HSO_5^-, the linear part of the oxygen induced step, described by k_0, should be retarded, as the results in Figures 13 and 14 clearly indicate. Thus the turnover from the exponential part to the linear part occurs, when $[SO_5^{\bullet-}]$ and the $[HSO_5^-]$ are large enough that the back-reaction (the oxidation of iron(II) to iron(III)) becomes dominant.

t_{bp} and k_0 show different behaviors in the presence of ethanol and hydroquinone, respectively. With increasing $[C_2H_5OH]$ both t_{bp} and k_0 reach a limiting value, whereas in the case of hydroquinone t_{bp} increases and k_0 decreases linearly with increasing $[C_6H_4(OH)_2]$. One reason for this difference could be the stability of the employed radical scavengers against oxygen. Hydroquinone can be oxidized by oxygen to quinone[77] (eq 5).

$$C_6H_4(OH)_2 + O_2 \rightarrow C_6H_4O_2 + H_2O_2 \qquad (5)$$

The oxygen consumption rate has been measured to be 2.2×10^{-8} M h^{-1} (pH 2.8, T = 25 °C) in the presence of iron(III).[78] Thus, the amount of oxygen consumed within the reaction time (20–50 s) is negligible compared to the oxygen consumption induced by sulfur(IV). On the other hand, high concentrations of ethanol can reduce the oxygen solubility, which in turn can result in a driving out of oxygen during the mixing process. Measurements with the oxygen electrode[42] indicate no change in $[O_2]$ with increasing $[C_2H_5OH]$ and no increase in the amount of consumed oxygen with increasing $[C_6H_4(OH)_2]$ under the selected reaction conditions. Thus the observed difference in the behavior of t_{bp} and k_0 with increasing $[C_2H_5OH]$ and $[C_6H_4(OH)_2]$, respectively, is not due to a change in the oxygen concentration at different radical scavenger concentrations. Comparison of the reaction rates for some sulfur–oxo radicals with hydroquinone and ethanol (Table 4) indicate that ethanol is a much poorer radical scavenger than hydroquinone. In the present work a ca. 1000 times higher ethanol concentration compared to hydroquinone was used, which is probably responsible for the different behavior and the more drastic effects induced by ethanol.

Modeling of Mechanism. For the model calculations a GEAR algorithm[79] based computer program[80] was used. For several reaction steps, the appropriate range of the rate constants were verified by systematically varying its value while keeping other parameters constant. The same sort of sensitivity analysis was used to eliminate kinetically insignificant reaction steps from the model. The most important aspects of the mechanistic considerations are discussed below.

We consider the deprotonated sulfito complexes, $Fe(SO_3)_n$, to be the dominant form under the selected conditions in this study (pH 2.5). Since our considerations refer to constant pH, no distinction is made between the alternative protonated forms of the sulfito complexes (see introduction). On the basis of the same argument, the protolytic equilibria involving sulfur(IV) are not included in the model. Sulfur(IV) is always written as HSO_3^-,

(77) James, T. H.; Snell, J. M.; Weissberger, A. *J. Am. Chem. Soc.* **1938**, *60*, 2084.
(78) Miles, C. J.; Brezonik, P. L. *Environ. Sci. Technol.* **1981**, *15*, 1089.
(79) Hindmarsh, A. C. GEAR: Ordinary differential equation system solver; Technical Report No. UCM-3001, Rev. 2; Lawrence Livermore National Laboratory, Livermore, CA, 1972.
(80) Peintler, G. ZITA 3.0: A comprehensive program package for fitting parameters of chemical reaction mechanisms, Szeged, Hungary, 1992.
(81) Conklin, M. H.; Hoffmann, M. R. *Environ. Sci. Technol.* **1988**, *22*, 899.
(82) Skorik, N. A.; Zatolokina, N. A. *Russ. J. Inorg. Chem. (Engl. Transl.)* **1986**, *31*, 1318.
(83) Stanbury, D. M. *Adv. Inorg. Chem.* **1989**, *33*, 69.
(84) Sarala, R.; Islam, M. S.; Rabin, S. B.; Stanbury, D. M. *Inorg. Chem.* **1990**, *29*, 1133.
(85) Sadat-Shafaï, T.; Pucheault, J.; Ferradini, C. *Radiat. Phys. Chem.* **1981**, *17*, 283.
(86) Behar, D.; Fessenden, R. W.; Hornak, J. P. *Radiat. Phys. Chem.* **1982**, *20*, 267.
(87) Eriksen, T. E. *J. Chem. Soc., Faraday Trans. 1* **1974**, *70*, 208.
(88) Bartels, D. M.; Lawler, R. G. *J. Chem. Phys.* **1987**, *86*, 4843.
(89) Behar, D.; Fessenden, R. D. *J. Phys. Chem.* **1972**, *76*, 1706.
(90) Buxton, G. V.; McGowan, S.; Salmon, G. A. In *Photo-oxidants: Precursors and products; Proceedings of EUROTRAC Symposium '92, Garmisch-Partenkirchen, Germany, 23rd-27th March 1992*; Borrell, P. M., Borrell, P., Cvitaš, T., Seiler, W., Eds.; SPB Academic Publishing: Den Haag, The Netherlands, 1993; pp 599–604.
(91) Huie, R. E.; Clifton, C. L.; Altstein, N. *Radiat. Phys. Chem.* **1989**, *33*, 361.
(92) Huie, R. E.; Neta, P. Poster presented at the Chemrawn VII conference, Dec 2–6, 1991, Baltimore, MD.
(93) Chawla, O. P. Ph.D. Thesis, Carnegie Mellon University, Pittsburgh, PA, 1973; cited in: Ross, A. B.; Neta, P. *NSRDS-NBS Report 65*; NBS: Washington, DC, 1979.
(94) Wine, P. H.; Tang, Y.; Thorn, R. P.; Wells, J. R. *J. Geophys. Res.* **1989**, *94(D1)*, 1085.
(95) Betterton, E. A.; Hoffmann, M. R. *J. Phys. Chem.* **1988**, *92*, 5962.
(96) Jacob, D. J. *J. Geophys. Res.* **1986**, *91(D9)*, 9807.
(97) Warneck, P. In *Laboratory Studies of the Aqueous Chemistry of Free Radicals, Transition Metals and Formation of Acidity in Clouds* Warneck, P., contract coordinator; Final Report Contract No. STEP-0005-C(MB), April 1, 1990–March 31, 1992; 1992; pp 1–10.
(98) Lee, Y. J.; Rochelle, G. T. *Environ. Sci. Technol.* **1987**, *21*, 266.
(99) Jayson, G. G.; Parsons, B. J.; Swallow, A. J. *J. Chem. Soc., Faraday Trans. 1* **1972**, *68*, 2053.
(100) Stuglik, Z.; Zargorski, Z. P. *Radiat. Phys. Chem.* **1981**, *17*, 229.
(101) Christensen, H.; Sehested, K. *Radiat. Phys. Chem.* **1981**, *18*, 723.
(102) Farhataziz; Ross, A. B. *Selected specific rates of reactions of transients from water in aqueous solution. III. Hydroxyl radical and perhydroxyl radical and their radical ions*; NSDRS-NBS 59; U.S. Dept. of Commerce: Washington, DC, 1977.
(103) Adams, G. E.; Boag, J. W. *Proc. Chem. Soc. London* **1964**, 112.
(104) Maruthamuthu, P.; Neta, P. *J. Phys. Chem.* **1977**, *81*, 937.

Table 5. Kinetic Model for the Iron(III)–Sulfur(IV)–Oxygen System[a,b]

Reaction	lit. values for the stability and rate const: const	lit. values for the stability and rate const: value	ref	stability and rate const used in the model
$Fe^{3+} + HSO_3^- \rightleftharpoons FeSO_3^+$ (6)	K_6	66.8 (pH 2.1)	81	600
		85 (pH 2.0)	82	
		108 (pH 2.1)	82	
		200 (pH 3.4)	82	
		600 (pH 2.5)	23	
		700 (pH 3.2)	82	
	k_6	270	60	600
	k_{-6}			1.0
$FeSO_3^+ \rightleftharpoons Fe^{2+} + SO_3^{\bullet-}$ (7)	k_7	2.1×10^{-3} (pH 2.0)	81	0.2
		0.14 (pH 2.5)	25	
		0.2 (pH 2.5)	*c*	
	k_{-7}	9.8×10^6 pH 4.0)	64	9.8×10^6
$Fe^{2+} + HSO_3^- \rightleftharpoons FeSO_3$ (8)	K_8	500 (pH 4.0)	64	16
	k_8			1.0×10^6
	k_{-8}			6.3×10^4
$FeSO_3 + SO_3^{\bullet-} \rightarrow Fe^{3+} + 2SO_3^{2-}$ (9)	k_9	3.2×10^6 (pH 4.0)	64	3.2×10^6
$Fe^{3+} + SO_3^{\bullet-} \rightarrow Fe^{2+} + SO_4^{2-}$ (10)	k_{10}			1.5×10^7
$SO_3^{\bullet-} + SO_3^{\bullet-} \rightarrow S_2O_6^{2-}$ (11)	K_{11}	1.0×10^{-19}	83	
		3.0×10^{-24}	84	
	$2k_{11}$	3.6×10^8 (pH 4.3)	26	1.0×10^9
		6.8×10^8 (pH 9.8)	85	
		7.2×10^8 (pH 10.7)	86	
		8.5×10^8 (pH 5.0)	87	
		1.1×10^9 (pH 9.8)	69	
		1.4×10^9 (pH 10.0)	87	
		1.6×10^9 (pH 14.0)	88	
		1.9×10^9 (pH 11.8)	89	
		2.3×10^9	90	
$SO_3^{\bullet-} + O_2 \rightarrow SO_5^{\bullet-}$ (12)	k_{12}	1.1×10^9 (pH ~ 1.0)	91	1.0×10^9
		1.2×10^9	29	
		1.5×10^9 (pH 6.8)	28	
		2.5×10^9	64	
$SO_5^{\bullet-} + HSO_3^- \rightarrow SO_3^{\bullet-} + HSO_5^-$ (13)	k_{13}	2.5×10^4 (pH 4.9)	30	5.0×10^4
		3.0×10^6 (pH 6.8)	28	
		1.3×10^7 (pH 8.7)	30	
$SO_5^{\bullet-} + HSO_3^- \rightarrow SO_4^{\bullet-} + HSO_4^-$ (14)	k_{14}	2.5×10^4 (pH 4.9)	30	5.0×10^4
		6.0×10^5	92	
		1.3×10^7	14	
$SO_4^{\bullet-} + HSO_3^- \rightarrow SO_3^{\bullet-} + HSO_4^-$ (15)	k_{15}	2.6×10^8 (pH 7–8)	93	8.0×10^8
		3.1×10^8 (pH 9.0)	90	
		3.8×10^8 (pH 9.0)	92	
		4.6×10^8	30	
		5.3×10^8 (pH > 7)	69	
		5.5×10^8 (pH 8.0)	29	
		7.5×10^8 (pH 4.8)	94	
		2.0×10^9 (pH 8.7)	30	
$HSO_5^- + HSO_3^- \rightarrow 2HSO_4^-$ (16)	k_{16}	3.5×10^2 (pH 8.0)	29	7.5×10^7
		9.1×10^3 (pH 2.9)	95	
		2.0×10^4 (pH 2.5)	95	
		7.9×10^4 (pH 1.5)	95	
		7.5×10^7	96	
$SO_5^{\bullet-} + SO_5^{\bullet-} \rightarrow 2SO_4^{\bullet-} + O_2$ (17)	$2k_{17}$	1.1×10^7 (pH 9.0)	92	1.0×10^9
		1.9×10^8	90	
		2.0×10^8	94	
		6.0×10^8	30	
$Fe^{2+} + SO_5^{\bullet-} \rightarrow Fe^{3+} + HSO_5^-$ (18)	k_{18}	2.0×10^8	54	1.0×10^7
$Fe^{2+} + HSO_5^- \rightarrow Fe^{3+} + SO_4^{\bullet-} + OH^-$ (19)	k_{19}	3.0×10^4	55	*d*
$Fe^{2+} + HSO_5^- \rightarrow Fe^{3+} + SO_4^{2-} + OH^{\bullet}$ (20)	k_{20}	3.0×10^4	97	*d*
$Fe^{2+} + SO_4^{\bullet-} \rightarrow Fe^{3+} + SO_4^{2-}$ (21)	k_{21}	4.0×10^7 (pH 2.1)	56	*d*
		8.6×10^8	98	
		9.9×10^8	73	
$Fe^{2+} + OH^{\bullet} \rightarrow Fe^{3+}$ (22)	k_{22}	2.3×10^8 (pH 1.0)	99	*d*
		3.2×10^8 (pH 7.0)	100	
		4.3×10^8 (pH 3.0)	101	
		5.0×10^8 (pH 2.0)	102	
$HSO_3^- + OH^{\bullet} \rightarrow SO_3^{\bullet-}$ (23)	k_{23}	2.7×10^9 (pH 4.5)	64	*d*
		4.1×10^9 (pH 9.0)	64	
		4.5×10^9 (pH 4.4)	30	
		4.6×10^9 (pH 9.0)	90	
		5.2×10^9 (pH 11.2)	30	
		9.5×10^9	103	
$HSO_5^- + OH^{\bullet} \rightarrow SO_5^{\bullet-}$ (24)	k_{24}	1.7×10^7 (pH 7.0)	104	*d*
$HSO_5^{\bullet-} + HSO_5^- \rightarrow SO_4^{\bullet-} + SO_4^{2-} + O_2$ (25)	$2k_{25}$	$10^7 - 10^{10}$ [e]		*d*
$SO_3^{\bullet-} + SO_5^{\bullet-} \rightarrow S_2O_6^{2-} + O_2$ (26)	k_{26}	$10^7 - 10^{10}$ [e]		*d*

[a] The reactions in the table are not balanced for H^+ and OH^-, because we want to emphasize the main reaction paths operative in the suggested mechanism. Furthermore all mechanistic considerations apply for a constant pH of 2.5. [b] First-order rate constants are in s^{-1}; second-order rate constants are in $M^{-1}\ s^{-1}$. [c] This work. [d] Reaction not included in the final model; see Discussion for details. [e] Since no literature data are available for these rate constants, the range of the sensitivity analysis is given.

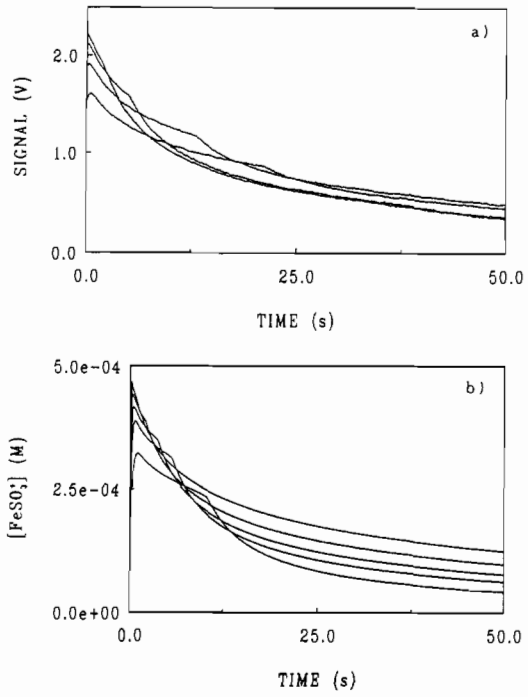

Figure 15. Effect of [S(IV)] on the overall reaction. (a) Experimental conditions: [Fe(III)] = 5.0×10^{-4} M; [O_2] = 7.5×10^{-4} M; μ = 0.5 M; T = 25 °C; pH = 2.5, λ = 390 nm; in order of increasing [$FeSO_3^+$], [S(IV)] = 5.0×10^{-3}, 1.0×10^{-2}, 2.5×10^{-2}, and 5.0×10^{-2} M. (b) Model conditions: [Fe(III)] = 5.0×10^{-4} M; [O_2] = 7.5×10^{-4} M; in the order of increasing [$FeSO_3^+$], [S(IV)] = 5.0×10^{-3}, 1.0×10^{-2}, 1.5×10^{-2}, 2.5×10^{-2}, and 5.0×10^{-2} M.

since this is the dominant S(IV) species under the conditions applied here. However, it needs to be emphasized that when the same model is adapted for the interpretation of the pH dependence of the overall reaction, these simplifications cannot be applied anymore.

Only the formation of $FeSO_3^+$ is assumed in the proposed model and the observed absorbance changes at λ = 390 nm are attributed to this species. This simplification implies that the redox reactions of the different iron(III)–sulfito complexes follow the same kinetic pattern, which was found to be the case.[25] The inherent limitations of this approach are obvious. Still, it seems to be permissible in the present system since the very general features of the experimental curves do not depend on the total sulfite ion concentration. For example, under all conditions a fast absorbance increase is observed (in less than 0.5 s) which is followed by a considerably slower decay (Figure 1). Also, when oxygen is added, the characteristic break-point in the kinetic curves (at the time t_{bp}) is detected in a wide range of S(IV) concentrations (Figure 15a).

Our proposed mechanism is mainly based on the work of Backström.[8] The detailed kinetic model is summarized in Table 5. If the proposed model is correct, it must predict similar concentration vs time profiles for the $FeSO_3^+$ complex as the experimentally observed absorbance–time traces (e.g. Figures 1–3).

As mentioned above, the reaction starts with the rapid formation of the $FeSO_3^+$ complex. The value of 600 M^{-1} [23] was used for the stability constant of the $FeSO_3^+$ complex throughout the calculations. The reported rate constant for the formation of this complex is 270 M^{-1} s^{-1}.[60] With this value the calculated complex formation is somewhat slower as observed and the maxima on the calculated concentration profiles are delayed compared to the experimental curves. An approximately 2-fold increase in the rate constant can resolve this discrepancy. The reverse rate constant for the same step was calculated from the forward rate constant and the equilibrium constant, $k_{-6} = k_6/K_6$.

The next step is the redox decomposition of $FeSO_3^+$, which produces the $SO_3^{\bullet-}$ radical (reaction 7). The rate constant of this step reportedly increases on increasing [S(IV)] and reaches a limiting value of 0.14 s^{-1} at [S(IV)] = 2.5×10^{-3} M.[25] From our experimental results we obtained a somewhat higher limiting rate constant, 0.2 s^{-1}. According to pulse radiolysis experiments,[64] the decomposition is reversible and the rate constant for the backward step is 9.8×10^6 M^{-1} s^{-1}. The complex equilibria between iron(II) and sulfur(IV) (reaction 8) have been investigated before. At pH = 4.0, the apparent stability constant for reaction 8 is K_8 = 500 M^{-1}.[64] From this, the estimated stability constant at pH = 2.5 is K_8 = 16 M^{-1}. The complex formation kinetics of this sulfito complex has not been studied before. On the basis of kinetic data for water exchange and ligand substitution reactions of iron(II), the formation rate constant is expected to be on the order of 10^6 M^{-1} s^{-1}.[105] Similar to the observation for iron(II), the corresponding sulfito complex also reacts with the $SO_3^{\bullet-}$ radical. The rate constant obtained by pulse radiolysis experiments[87] for this step (eq 9) is 3.2×10^6 M^{-1} s^{-1}.

The main sulfur-containing product of the overall reaction is sulfate ion. It was confirmed that reaction 27 cannot be the main source of SO_4^{2-}. Even when a diffusion-controlled rate constant

$$SO_3^{\bullet-} + SO_3^{\bullet-} \rightarrow SO_2 + SO_4^{2-} \quad 2k_{27} = 2.3 \times 10^8\ M^{-1}\ s^{-1}\ [26] \tag{27}$$

is assumed for this step (10^{10} M^{-1} s^{-1}) the calculations predict an unrealistically slow decomposition of $FeSO_3^+$. It needs to be emphasized that, on the basis of previous literature,[26] the estimated value for k_{27} is about 2 orders of magnitude below the diffusion controlled limit. These results imply that the $SO_3^{\bullet-}$ radical is oxidized by some iron(III) species, presumably by $Fe(H_2O)_6^{3+}$. Reaction 10 seems to be one of the key steps.[43] A similar reaction step was postulated in the autoxidation of sulfite ion in the presence of copper(III)[5] and nickel(III) complexes.[106] By following the considerations of Anast and Margerum,[5] reaction 10 corresponds to the following reaction sequence.

$$Fe^{3+} + SO_3^{\bullet-} \rightleftharpoons Fe^{2+} + SO_3 \tag{28}$$

$$SO_3 + H_2O \rightleftharpoons H_2SO_4 \tag{29}$$

$$H_2SO_4 \rightleftharpoons SO_4^{2-} + 2H^+ \tag{30}$$

After the maximum $FeSO_3^+$ concentration is reached, the shape of the kinetic curves is determined by the competition of reaction 10 with other reactions of the $SO_3^{\bullet-}$ radical. Significant deviation from first-order behavior was observed only in the last 20–25% of the experimental curves. This deviation is the consequence of the reoxidation of iron(II) species to iron(III) (reactions 7, 9, and 18–22). It follows that reaction 10 must dominate over these steps for up to 75–80% of the overall reaction. Since no literature data are available for reaction 10, the rate constant, k_{10}, must be carefully selected in order to simulate this feature. According to a sensitivity analysis, a value of the order of 10^7 M^{-1} s^{-1} seems to be consistent with the experimental observations. In subsequent calculations, $k_{10} = 1.5 \times 10^7$ M^{-1} s^{-1} was used.

In the absence of oxygen, the overall reaction can be properly described with reactions 6–11. Reaction 11 needs to be included in order to account for the formation of $S_2O_6^{2-}$, which was experimentally observed at different concentration levels.[1,25,29,67] In the presence of oxygen, the redox cycle is controlled by the formation of the peroxomonosulfate radical, $SO_5^{\bullet-}$ (12). This species is a much more reactive oxidant ($E°(SO_5^{\bullet-}/HSO_5^-)$ = 1.1 V, pH = 7[28]) than O_2 ($E°(O_2/O_2^{\bullet-})$ = –0.33 V, pH = 7,

(105) Margerum, D. W.; Cayley, G. R.; Weatherburn, D. C.; Pagenkopf, G. K. In *Coordination Chemistry, Vol. 2*; Martell, A. E., Ed.; American Chemical Society: Washington, DC, 1978; pp 1–220 and references therein.

(106) Linn, D. E., Jr.; Dragan, M. J.; Miller, D. E. *Inorg. Chem.* **1990**, *29*, 4356.

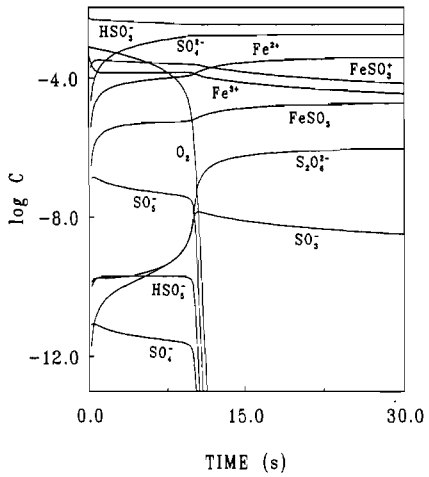

Figure 16. Simulated concentration–time profiles for the iron(III)-catalyzed autoxidation of sulfur(IV) oxides. Conditions: [Fe(III)] = 5.0×10^{-4} M; [S(IV)] = 5.0×10^{-3} M; [O_2] = 7.5×10^{-4} M; stability and rate constants from Table 5.

$E°(O_2/H_2O_2) = 0.28$ V, pH = 7)[107] and may oxidize either sulfite ion (reactions 13 and 14) or iron(II) (reaction 18). The produced sulfate radical, $SO_4^{\bullet-}$ (reaction 14) can induce several oxidation processes ($E°(SO_4^{\bullet-}/SO_4^{2-}) = 2.43$ V[83]), e.g., oxidizing either the sulfite ion (reaction 15) or iron(II) (reaction 21). Because of the excess of sulfur(IV) and iron(II) compared to the [$SO_4^{\bullet-}$], a recombination of the sulfate radical (reaction 31) is unlikely and is not included in the model.

$$SO_4^{\bullet-} + SO_4^{\bullet-} \rightarrow S_2O_8^{2-} \quad 2k = 3.8 \times 10^8 - 3.6 \times 10^9\ M^{-1}\ s^{-1}\ ^{56,74,92,108,109} \quad (31)$$

The hydrogen peroxomonosulfate anion, HSO_5^-, formed in reactions 13 and 18 together with the peroxomonosulfate radical, $SO_5^{\bullet-}$, opens various reaction pathways that may influence both the decomposition process and the product formation. A thorough inspection of the model reveals that under the conditions considered here ([HSO_3^-] > [Fe(II)]) (20) is inferior to (16). Because of the more than 3 orders of magnitude difference in the corresponding rate constants, hydroxyl radicals are produced at extremely low concentration levels. Thus, all reaction steps which include this species can be rejected from the model. Similarly, reaction 10 is considerably faster than (21), and the latter step can be eliminated. On the basis of analogous considerations, steps (25) and (26) can also be excluded. Model calculations confirmed these conclusions. The simulated kinetic curves were identical regardless whether reactions 19–26 were included in the model or not.

Thus steps 6–18 summarized in Table 5 represent a basic set of reactions which are required for the proper interpretation of the overall reaction. The calculated concentration-time profiles for various species in this system are shown in Figure 16. The [Fe(III)] drops in the first few seconds of the reaction because of the formation of the $FeSO_3^+$ complex. The concentration profiles of both iron(III) and the $FeSO_3^+$ complex are nearly constant since dissolved oxygen is still left in the system and the produced $SO_5^{\bullet-}$ radical oxidizes iron(II) back to iron(III) (step 18). The latter species again forms the iron(III)–sulfito complex (step 6), completing the catalytic cycle. When the dissolved oxygen in the system is used up, the concentrations of the oxygen-induced species, $SO_5^{\bullet-}$, (step 12), HSO_5^- (steps 13 and 18), and

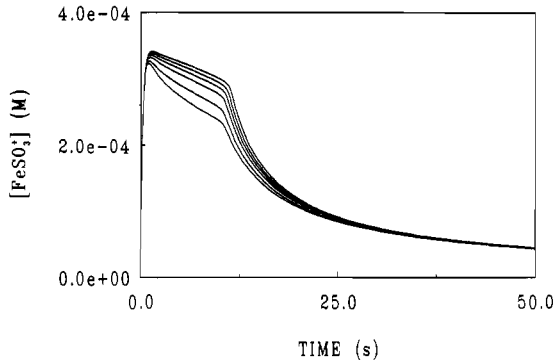

Figure 17. Result of the sensitivity analysis for reaction 18. k_{18} values in order of increasing [$FeSO_3^+$]: 1.0×10^7, 2.0×10^7, 5.0×10^7, 1.0×10^8, 2.0×10^8, and 5.0×10^8 M^{-1} s^{-1}.

$SO_4^{\bullet-}$ (step 14) decrease rapidly. The $SO_3^{\bullet-}$ concentration increases, because reaction 12 is no longer active.

As discussed above, the most important chain carrier is the $SO_3^{\bullet-}$ radical. In the absence of oxygen, this species is mainly consumed in the oxidation reaction with iron(III) (eq 10). In the presence of oxygen, the $SO_5^{\bullet-}$ radical opens a redox cycle by oxidizing sulfite ion. Since $SO_3^{\bullet-}$ is rapidly regenerated in (13) or (14) and (15), this reaction sequence cannot be responsible for the retarded decomposition rate of $FeSO_3^+$. The alternative path with iron(II), (18), regenerates iron(III). More importantly, the subsequent reaction step with HSO_5^- (eq 16) does not produce reactive chain carriers. Accordingly, reactions 16 and 17 result in the termination of the redox cycle and prevent further reduction of iron(III); i.e., the disappearance of the sulfito complex becomes slower. Indeed, when the kinetic importance of reaction 18 is increased compared to reactions 13 and 14, the decomposition before the break point becomes considerably slower (Figure 17). It should be noticed, that the reaction time where the break point occurs, is only slightly affected by the value of k_{18}. This is due to the fact that the oxygen consumption is primarily controlled by reaction 12.

The results obtained with the model are in good agreement with the experimental results (Figures 15 and 18–20), indicating the validity of the model.

Discussion

Kinetic modeling plays an important role in developing the reaction mechanisms for complex reaction systems.[12,110–112] The limitations of this technique are generally determined by the availability of reliable sets of rate constants for the applied conditions. The most common source of the ambiguity in the kinetic parameters is due to the evaluation of the experimental data based on simplified kinetic models. Quite often there is strong kinetic coupling between the individual reaction steps, and the simplifications result in biased estimates for the rate constants. As long as the kinetic parameters are determined on the basis of the same approximations, the results from different laboratories are generally consistent with each other. In contrast, different kinetic models may lead to conflicting results. Due to this problem, the rate constants may grossly be under- or overestimated in complicated systems. Recently, it has been demonstrated that in the case of complex reactions only systematic sensitivity analysis of the rate constants may justify the simplifications of the mechanism.[113,114]

(107) Sawyer, D. T. *Oxygen Chemistry*; Oxford University Press: New York, Oxford, England, 1991.
(108) Lesigne, B.; Ferradini, C.; Pucheault, J. *J. Phys. Chem.* **1973**, *77*, 2156.
(109) Tang, Y.; Thorn, R. P.; Mouldin, R. L., III; Wine, P. H. *J. Photochem. Photobiol., Part A* **1988**, *44*, 243.
(110) von Piechowski, M.; Nauser, T.; Hoigné, J.; Bühler, R. E. *Ber. Bunsen-Ges. Phys. Chem.* **1993**, *97*, 762.
(111) Warshel, A. *Computer Modeling of Chemical Reactions in Enzymes and Solutions*; John Wiley & Sons: New York, 1991.
(112) Chelkowska, K.; Grasso, D.; Fábián, I.; Gordon, G. *Ozone Sci. Eng.* **1992**, *14*, 33.
(113) Fábián, I.; Gordon, G. *Inorg. Chem.* **1992**, *31*, 2144.

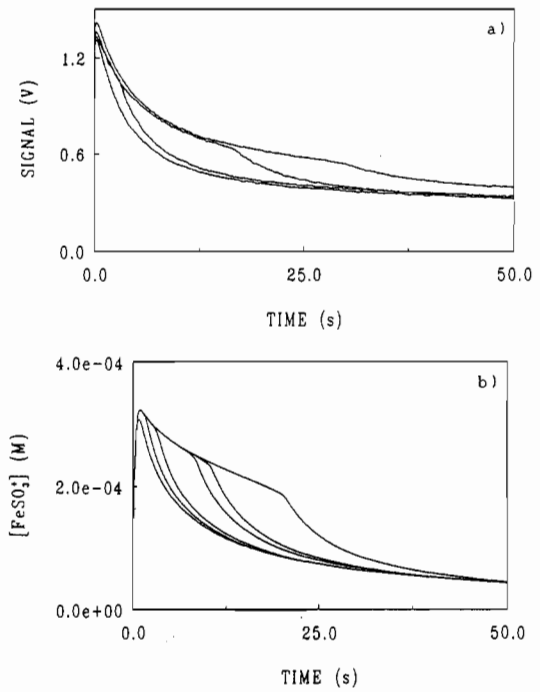

Figure 18. Effect of $[O_2]$ on the overall reaction. (a) Experimental conditions: $[Fe(III)] = 5.0 \times 10^{-4}$ M; $[S(IV)] = 7.5 \times 10^{-4}$ M; $\mu = 0.5$ M; $T = 25$ °C; pH = 2.5; $\lambda = 390$ nm; in order of increasing $[FeSO_3^+]$, $[O_2] = 0$, 2.6×10^{-4}, 7.5×10^{-4}, and 1.25×10^{-3} M. (b) Model conditions: $[Fe(III)] = 5.0 \times 10^{-4}$ M; $[S(IV)] = 5.0 \times 10^{-3}$ M; in the order of increasing $[FeSO_3^+]$, $[O_2] = 0$, 1.3×10^{-4}, 2.6×10^{-4}, 6.25×10^{-4}, 7.5×10^{-4}, and 1.25×10^{-3} M.

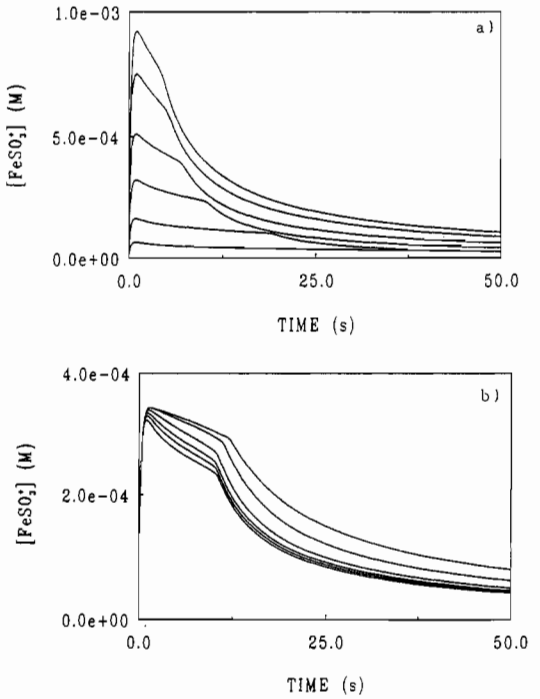

Figure 19. Simulated effect of (a) [Fe(III)] and (b) [Fe(II)] on the overall reaction. Conditions: (a) $[S(IV)] = 1.0 \times 10^{-2}$ M, $[O_2] = 7.5 \times 10^{-4}$ M, and in the order of increasing $[FeSO_3^+]$, $[Fe(III)] = 1.0 \times 10^{-4}$, 2.5×10^{-4}, 5.0×10^{-4}, 8.0×10^{-4}, 1.0×10^{-3}, and 1.2×10^{-3} M; (b) $[Fe(III)] = 5.0 \times 10^{-4}$ M, $[S(IV)] = 1.0 \times 10^{-2}$ M, $[O_2] = 7.5 \times 10^{-4}$ M, and in the order of increasing $[FeSO_3^+]$, $[Fe(II)] = 0$, 2.5×10^{-5}, 5.0×10^{-5}, 1.0×10^{-4}, 2.5×10^{-4}, and 5×10^{-4} M.

In principle, the model calculations can also be combined with appropriate fitting procedures in order to obtain the best estimates

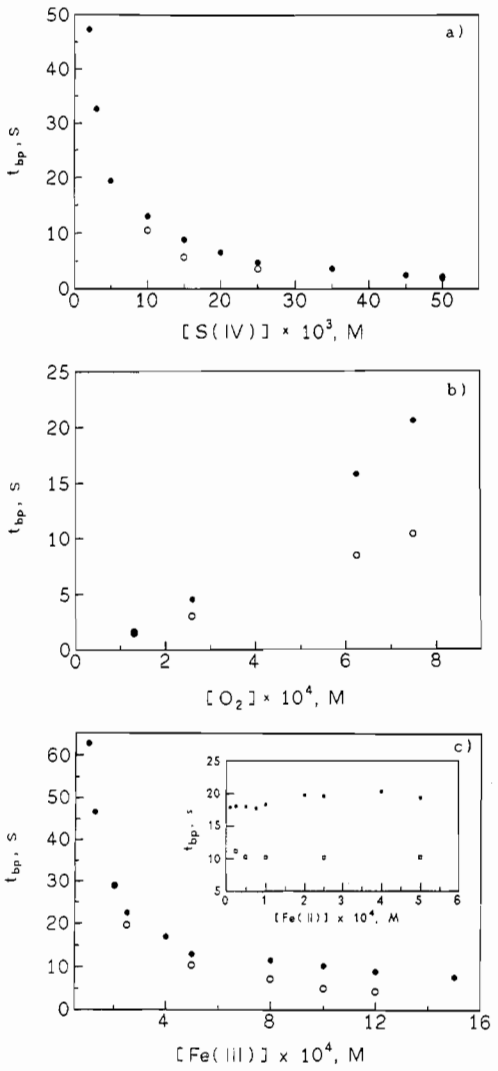

Figure 20. Comparison between model and experimental results for the dependence of t_{bp} on various experimental parameters. (a) [S(IV)] dependency (for conditions see Figure 15); (b) $[O_2]$ dependence (for conditions see Figure 18); (c) [Fe(III)] and [Fe(II)] dependence. For experimental conditions see Figure 19. In all cases: closed symbols are experimental values, open symbols are values predicted by the model.

for the rate constants.[80,115,116] However, because of the lack of sufficiently detailed experimental information, this procedure is usually not feasible. Accordingly, kinetic modeling typically yields a semiquantitative description of the studied systems; i.e., only rough estimates can be obtained for the lifetimes of the overall reactions. Therefore, the main objectives are (i) to properly simulate the general features and concentration dependencies of the experimental traces, (ii) to determine the main pathways in the intrinsic mechanism, and (iii) to design new experiments in order to clarify certain details of the overall reaction.

For the iron(III) catalyzed autoxidation of sulfur(IV) oxides, the simulated kinetic traces presented here follow similar trends to those observed experimentally. While the simulated concentration dependencies (Figures 15b, 18b, and 19) are qualitatively in good agreement with the experimental results (Figures 15a and 18a), the calculations predict a faster than observed decrease in the $[FeSO_3^+]$. Also, the concentration of the minor product $S_2O_6^{2-}$ is somewhat underestimated.

It needs to be emphasized that kinetic data are not available from the literature for all reaction steps, and most rate constants

(114) Gordon, G.; Fábián, I. *The Role of Highly Reactive Intermediates in the Decomposition of Aqueous Ozone, 10th Ozone World Congress and Exhibition*, Monaco, 1991; Vol. I, pp 113–124.

(115) Peintler, G.; Nagypál, I.; Epstein, I. R. *J. Phys. Chem.* **1990**, *94*, 2954.
(116) Weber, C. F.; Beahm, E. C.; Watson, J. S. *Comput. Chem.* **1992**, *16*, 325.

were published for experimental conditions that differ from ours (see Table 5). For example, there is a lack of literature data for reaction 10, and the rate constants for the reactions with iron(II) species (reactions 8, 9, and 18–22) should be considered as rough estimates. In addition, one of the main variables in this system is the pH, which controls the speciation[14] and the redox potential.[28,117] The main form of sulfur(IV) in the alkaline pH region is the SO_3^{2-} ion. In the copper(III)-catalyzed and the ozone-induced oxidation process, it is more reactive than HSO_3^-,[5,118] which is dominant at $2.5 \leq pH \leq 5.5$. In contrast, the reaction of H_2O_2 is faster with HSO_3^- than with SO_3^{2-}.[119] Finally, in the transition metal catalyzed oxidation of sulfur(IV) oxides often a bell-shaped pH dependence has been observed,[6,67,82,120,121] which complicates matters even further. Thus, it is difficult to predict a simple trend in the rate constants by comparing the values under different conditions. For most of the rate constants, the confirmation of the actual value at pH 2.5 would require a detailed study of the pH profile.

Furthermore, some of the reactions included in the model are most likely the composite of various elementary steps. An example is reaction 16, which may proceed through a multistep reaction mechanism[95,122] with the disulfate ion, $S_2O_7^{2-}$, as intermediate. Reaction 16 may represent the following reaction sequence:[122]

$$HSO_3^- + HSO_5^- \rightarrow O_3SOOSO_2^{2-} + H_2O \quad (32)$$

$$O_3SOOSO_2^{2-} + H^+ \rightarrow O_3SOSO_3^{2-} + H^+ \quad (33)$$

$$O_3SOSO_3^{2-} + H_2O \rightarrow 2SO_4^{2-} + 2H^+ \quad (34)$$

Disulfate ion, $S_2O_7^{2-}$, is a known intermediate in the uncatalyzed oxidation of sulfite ion by oxygen.[123,124] To the best of our knowledge, no information on a possible influence of this species on the transition metal catalyzed autoxidation of sulfur(IV) oxides has been reported. Nevertheless, disulfate ion and other intermediates formed in composite steps may react with the reactants and each other, thus, affecting the course of the overall reaction.

Finally it should be added, the reaction products SO_4^{2-} and $S_2O_6^{2-}$ have at most marginal effects on the catalytic autoxidation of sulfur(IV) oxides[67] in the studied concentration range. Accordingly, the inclusion of additional steps with these ions would not improve the proposed model. The shortcomings discussed above inevitably introduced certain ambiguity into the calculations and better agreement between the calculated and experimental kinetic curves could not be achieved.

For a variety of conditions, the experimental and simulated kinetic curves are compared in Figures 15 and 18. As shown, when [S(IV)] is increased (Figure 15), the reaction in the oxygen induced phase becomes faster and eventually, at high [S(IV)], the break point at t_{bp} disappears. This is the consequence of accelerating the propagation steps with HSO_3^- compared to the regeneration of the iron(III)–sulfito complex via reactions 6, 9, and 18. The [S(IV)] dependence exhibits very good agreement between the model and the experimental results (Figure 15).

As shown in Figure 18, the rate of the oxygen-induced phase is practically not affected by the oxygen concentration. Apparently, the amount of the added oxygen determines only the length of this region, i.e. t_{bp}. This strongly suggests that reaction 12 is not the rate-determining step in the mechanism. The plot of t_{bp} as a function of the oxygen concentration (Figure 20b) reveals that both the calculated and experimental values increase exponentially with increasing $[O_2]$. Although the calculated oxygen consumption is somewhat faster than observed, the model yields an excellent prediction for the $[O_2]$ dependence.

The simulated [Fe(III)] and [Fe(II)] dependencies (Figure 19) describe the experimentally observed behavior very good. When [Fe(III)] is increased, the concentration of the sulfito complex is increased. This accelerates the catalytic cycle, and the oxygen consumption becomes considerably faster. After all the oxygen is consumed (at the time t_{bp}), the decomposition follows approximately first-order kinetics which is independent of the initial [Fe(III)]. This is in excellent agreement with the results obtained from separate experiments in the absence of oxygen.

Iron(II) has a retarding effect on the oxygen-induced phase of the reaction and the t_{bp} values reach a limiting value as a function of [Fe(II)] (Figure 20c). The kinetic role of iron(II) can be understood by considering that the increase in [Fe(II)] increases the rate of reaction 18. As demonstrated earlier, when this step is accelerated compared to reactions 13 and 14 the decomposition becomes retarded in the presence of oxygen. When [Fe(II)] is increased, the roughly exponential profile of the oxygen induced region changes gradually. Above [Fe(II)] of 10^{-4} M the traces show zero-order kinetics. Similar to iron(III), following the break point the kinetics is slightly affected by iron(II). These features are predicted very well by the proposed model.

Conclusions

The qualitative mechanistic interpretation reported above offers a simple and logic explanation for the occurrence of the peculiar and additional reaction step in the presence of oxygen. Thus there is no need to suggest the participation of oxo complexes as we have done before[25] or as it is reported in the literature.[1,49,50] The sulfite-induced autoxidation of iron(II) to iron(III), which will subsequently rapidly coordinate the excess sulfite, can account for the formation of the break point in the absorbance time traces. Thus the redox cycling of iron in the presence of sulfite and oxygen[65] can account for all the observations made in this study. As soon as the O_2 concentration is reduced to zero, no oxidation of iron(II) can occur and the normal reduction of iron(III) by sulfite continues to completion. The suggested mechanism is in line with that proposed for the transition metal catalyzed sulfur(IV) oxidation in recent literature[5,6,9,12,106] and forms the basis for the simulation of the overall mechanism.

Iron(II) is oxidized by the $SO_5^{\bullet-}$ radical (or its reaction products) in the presence of oxygen. The decomposition of the $FeSO_3^+$ complex is determined by the competition between reaction 10 and other reactions of the sulfite radical ion, $SO_3^{\bullet-}$. The distinct part of the oxygen induced step before the break point is due to the reoxidation of iron(II) species to iron(III).

Further experimental work should be directed to distinguish the kinetic role of various iron(III)–sulfito complexes, to a systematic study of pH effects, and to obtain better defined kinetic parameters for the individual reaction steps. Most importantly, the conclusions regarding the value of k_{10} should be confirmed experimentally.

Acknowledgment. The authors gratefully acknowledge financial support from the Deutsche Forschungsgemeinschaft, Bundesministerium für Forschung und Technologie, and Commission of the European Community (STEP Programme). The award of a research fellowship by the Alexander von Humboldt Foundation to I.F. is greatly appreciated.

(117) Latimer, W. M. *Oxidation Potentials*, 2nd ed.; Prentice Hall: Englewood Cliffs, NJ, 1952.
(118) Hoigné, J.; Bader, H.; Haag, W. R.; Staehlin, J. *Water Res.* **1985**, *19*, 993.
(119) McArdle, J. V.; Hoffmann, M. R. *J. Phys. Chem.* **1983**, *87*, 5425.
(120) Ibusuki, T.; Takeuchi, K. *Atmos. Environ.* **1987**, *21*, 1555.
(121) Grgić, I.; Hudnik, V.; Bizjak, M.; Levec, J. *Atmos. Environ.* **1992**, *26A*, 571.
(122) Connick, R. E.; Lee, S.; Adamic, R. *Inorg. Chem.* **1993**, *32*, 5962.
(123) Chang, S.-G.; Littlejohn, D.; Hu, K. Y. *Science* **1987**, *237*, 756.
(124) Littlejohn, D.; Hu, K. Y.; Chang, S.-G. *Ind. Eng. Chem. Res.* **1988**, *27*, 1344.